Dynamic programming-based multi-vehicle longitudinal trajectory optimization with simplified car following models

Author list

Yuguang Wei[a], Cafer Avcı[b,c,e], Jiangtao Liu[c], Baloka Belezamo[c,d], Nizamettin Aydın[e], Pengfei (Taylor) Li[f], Xuesong Zhou [c,*]

[a]*School of Traffic and Transportation, Beijing Jiaotong University, Beijing, 100044, China*
[b]*Computer Engineering Department, Faculty of Engineering, Yalova University, Yalova, 77200, Turkey*
[c]*School of Sustainable Engineering and the Built Environment, Arizona State University, Tempe, AZ 85281, USA*
[d]*Arizona Department of Transportation (ADOT), Phoenix, Arizona, 85007, USA*
[e] *Computer Engineering Department, Faculty of Electrical and Electronics, Yıldız Technical University, Istanbul, 34220, Turkey*
[f] *Department of Civil & Environmental Engineering, Mississippi State University, Mississippi State, MS 39762, USA*

Abstract

Jointly optimizing multi-vehicle trajectories is a critical task in the next-generation transportation system with autonomous and connected vehicles. Based on a space-time lattice, we present a set of integer programming and dynamic programming models for scheduling longitudinal trajectories, where the goal is to consider both system-wide safety and throughput requirements under supports of various communication technologies. Newell's simplified linear car following model is used to characterize interactions and collision avoidance between vehicles, and a control variable of time-dependent platoon-level reaction time is introduced in this study to reflect various degrees of vehicle-to-vehicle or vehicle-to-infrastructure communication connectivity. By adjusting the lead vehicle's speed and platoon-level reaction time at each time step, the proposed optimization models could effectively control the complete set of trajectories in a platoon, along traffic backward propagation waves. This parsimonious multi-vehicle state representation sheds new lights on forming tight and adaptive vehicle platoons at a capacity bottleneck. We examine the principle of optimality conditions and resulting computational complexity under different coupling conditions.

Keywords: Traffic flow management, autonomous vehicle, vehicle trajectory optimization, car-following model

[*] Corresponding author. Tel.: +1 480 9655827.
E-mail addresses: ygwei@bjtu.edu.cn (Y. Wei), cafer.avci@yalova.edu.tr (C. Avcı), jliu215@asu.edu (J. Liu), bbelezamo@adot.gov (B.Belezamo), naydin@yildiz.edu.tr (N. Aydın), pengfei.li@cee.msstate.edu (P. Li), xzhou74@asu.edu (X. Zhou).

1. Introduction

As population, economic growth and personal travel activities continue to increase, traffic congestion remains as an extremely challenging problem due to limited road capacity and limited budgets for expanding infrastructure. A recently emerging technology, autonomous vehicles or automated vehicles (AV) are likely to create a revolutionary paradigm shift in the near future for real-time traffic system automation and control. AV technology is expected to provide a wide range of new opportunities for managing transportation networks, and also redefines what is tractable regarding full system-wide optimization through a tight integration among vehicles and system managers.

Varaiya (1993) outlined an automated highway systems (AHS) to significantly improve highway capacity and safety, in which a hierarchical control mechanism for AVs is provided at different spatial scales, ranging from a network, routes, freeway corridors, to dedicated lanes. In a recent review from the perspective of traffic flow theory and operations, Mahmassani (2016) highlighted many unique features and challenges in the next-generation transportation systems of optimizing and controlling automated and connected vehicles. In the connected environment with different degrees of automation and connectivity supports, we need to not only fully recognize the changing driver/vehicle behavior (including car following and lane-changing), but also design a system-optimal scheduling and control architecture to achieve robust, stable and effective traffic flow management.

In our research, we focus on a longitude vehicle trajectory optimization problem, which is fundamental to many AV applications, such as vehicle platooning or adaptive cruise control. We briefly review the related research topics, including car following models and traffic-flow oriented trajectory optimization.

1.1 Review of car-following models and AVs' impact on traffic flow characteristics

Since the 1950s, there are a wide range of car following models proposed for vehicles driven by humans. After the earliest car-following models developed by Reuschel (1950) and Pipes (1953), many car-following models were developed based on the response-stimulus mechanism between a lead vehicle and a following vehicle. As examples, Kometani and Sasaki (1958, 1959, 1961), Forbes et al. (1958), Forbes (1963), and Chandler et al. (1958) had developed nonlinear car-following models, respectively. To overcome the complexity of those nonlinear models, Newell (1993, 2002) first presented a simplified car-following theory which is consistent with the macroscopic triangular flow-density relationship. Due to its simplicity without loss of flexibility, the Newell's simplified car-following models have been calibrated in many locations using real-world trajectory data. For example, Ahn el al. (2004) calibrated the Newell's car-following model using real-world vehicle trajectory data at signalized intersections. Taylor et al. (2015) applied the time-warping approach to investigate drivers' situation-dependent perception and reaction to external impetus. In parallel, there are also many studies focusing on calibrating various stochastic and situation-dependent car-following models, to name a few, Hamdar et al. (2009), Laval and Leclercq (2010), Hoogendoorn et al. (2011) and Kim and Mahmassani (2011).

While most car-following models focus on human-operated vehicles, researchers in automated control and artificial intelligence started characterizing the driving behaviors of AVs and their potential impact on road capacity in the 1990s. Reliable actuators and sensors in AVs, as summarized by Ward (1997), have made AVs more available and ready for field tests. There are two types of research efforts in parallel along this research line: one focusing on the interactions between AVs based on vehicle dynamics to derive possible changes to traffic characteristics; the other focusing on overall changes to the performance of road capacities brought by AVs under various conditions. As examples of the first type of research, Horowitz and Varaiya (2000) described the findings from the automated highway system (AHS) development in the 1990s at the California PATH program. In general, the actuators make AVs react much faster than a normal

or even sensitive human driver. Sensitive drivers can have a short perception-reaction time of 1.0 s to 1.5 s, as reported by NAHSC (1996), compared to a typical perception-reaction time of 2.0-2.5 s. Further shorter AV reaction times, such as 0.7 s reported by Bose and Ioannou (1999), can lead to closer spacing between cars and a higher roadway capacity. Another important aspect that motivates the development of AHS is based on optimal flow control through reducing or smoothing random errors in human drivers via the deterministic and possibly optimized vehicle trajectory planning/control. An early prototype for single-lane vehicle platooning on automated highways was reported by Alvarez and Horowitz (1999). They designed a safe zone between two platoons according to the distance, relative speed and maximum acceleration and deceleration rates. Horowitz and Varaiya (2000) also evaluated many platooning methods in simulation as well as in the physical test beds. Recently, Lioris et al. (2017) demonstrate that platoons of connected vehicles can double throughput in urban roads based on by the analysis of three queuing models and by the simulation of a road network with 16 intersections and 73 links.

A set of adaptive cruise controller (ACC) and the intelligent driver model controller (IDM by Treiber et al., 2000) were tested by Milanés and Shladover (2014) in different traffic situations in order to measure the actual responses of the vehicles. Talebpour and Mahmassani (2015) proposed a non-linear acceleration framework for autonomous vehicles and evaluated the possible changes to traffic flow stability. Roncoli et al. (2015a, 2015b) proposed a linear lane-based traffic flow model and discussed how to calibrate the model and optimize the traffic flow in the presence of autonomous vehicles. Using the relaxed Pontryagin's minimum principle, Hu et al. (2016) proposed an optimal controller to improve fuel efficiency for a vehicle equipped with automatic transmission traveling on rolling terrain. Recently, by applying the Improved Intelligent Driver Model (IIDM) in a road traffic simulation package named SUMO, Askari et al. (2017) assess the impact of the maximum vehicle acceleration and variable proportions of adaptive cruise control (ACC) and cooperative adaptive cruise control (CACC) vehicles on the throughput of an intersection. The results show that (C)ACC vehicles can obviously increase the urban mobility with little or no cost in infrastructure.

1.2 Review of vehicle trajectory optimization models

Vehicle trajectory optimization and control has been extensively studied in a broader domain, including surface vehicles, aircraft and Unmanned Aerial Vehicles (UAV). As summarized by Betts (1998), nonlinear programming, optimal control, and dynamic programming are classical modeling approaches to describe vehicle dynamics with various constraints and boundary conditions. Typical solution algorithms for single-vehicle trajectory optimization problems include direct shooting, indirect shooting, multiple shooting and direct/indirect transcription, where the last two methods aim to solve multipoint boundary value problems. By using a constrained optimization method on fuel consumption, He et al. (2015) proposed an approximation approach for providing advisory speed limit to drivers in the bottleneck. Along this line, Wu et al. (2015) applied reduce electricity consumption of electric vehicles method in the intersection. Focusing on the multi-vehicle trajectory coordination problem, Schouwenaars et al. (2001) proposed a mixed integer linear programming (MILP) model to use readily available linear programming or integer programming solvers such as CPLEX. In their proposed model, a set of vehicles move from initial boundary states to final states, subject to obstacle and inter-vehicle collision avoidance constraints. Recent development along this line can be found in the studies by Grotli and Johansen (2012), Richards et al. (2002) and Grotli and Johansen (2016) for UAV trajectory coordination problems, which cover a richer set of vehicle dynamics, obstacle avoidance, task timing requirement and communication-connectivity constraints. In mobile leader–follower networks, Sun and Cassandras (2016) highlights the important features of continuously preserving connectivity in a convex mission space.

Dynamic programming (DP)-based algorithms have been one key theoretic foundation for single-vehicle trajectory optimization, and its formulation typically involves several modeling elements: (i) the boundary of the search scope or map, (ii) discretized space-time lattices, (iii) a path searching algorithm that can find a safe trajectory to reach the destination and meet certain global goals, such as minimal fuel consumption or minimal travel times. While the DP-based trajectory optimization can reach the exact optimum, it is often too slow for real-time applications involving multiple vehicles. To address this issue, Flint et al. (2002) proposed an approximate DP algorithm for multiple vehicles to cooperatively search for targets. The dissertation by McNaughton (2011), based on an AV system architecture described by Urmson et al. (2008) for the 2007 DARPA Urban Challenge (DUC), proposed a novel five-dimensional search algorithm that recognizes kinematic and dynamic constraints in clearly defined spatial and temporal dimensions, and used graphics processing unit (GPU) to enable parallel search algorithms. Recent survey papers by Katrakazas et al. (2015) and Paden et al. (2016) reviewed the existing motion planning approaches for self-driving vehicles.

In a very recent study by Zhou et al. (2017), they proposed a shooting heuristic algorithm to smooth trajectories of multiple automated and connected vehicles, where a time geography-oriented approach is innovatively combined with Newell's simplified car following model to consider safe vehicle driving boundaries. Ma et al. (2016) further discussed the computational complexity and performance of their shooting algorithm in their preceding study. Bang and Ahn (2017) proposed an innovative framework to embed Newell's simplified car-following model with different reaction times for connected and autonomous vehicles (CAV) in a spring-mass-damper system (Yanakiev and Kanellakopoulos, 1998; Munigety et al., 2016). Their proposed swarm intelligence model is able to systematically characterize CAV platoon formation and evolution, under light traffic conditions. Gong et al. (2016) recently developed a rigorous convex program with quadratic constraints for representing the nonlinear safety distance constraint among coupled vehicles. To address the computational challenges, they used dual based distributed algorithms to iteratively refine the trajectory solutions and capture the desired transient and asymptotic dynamics. Compared these recent studies, our paper focuses on how to develop (linear) integer programming and dynamic programming model in a discretized multi-vehicle space-time representation. The parsimonious coupled multi-vehicle state representation to be constructed aims to not only shed new lights on defining the transient dynamic progress for adaptive vehicle platoons, but also provide a traffic-flow-oriented modeling methodology for extending a wide range of dynamic programming based real-time vehicle trajectory control algorithms under heaving and light traffic conditions.

In many multi-robot path planning applications, a group of autonomous vehicles follow predefined trajectories moving in a formation, which offers many advantages such as reducing team-level cost, increasing the robustness, efficiency and flexibility of the system. Designing such a system in a dynamic environment with avoiding obstacles to make motion planning requires robust configuration and discrete transformations (LaValle, 2006). Survey papers by Murray (2007) and Chen & Wang (2005) review the cooperative control and formation control of multi-vehicles/robots. With global and individually defined goals with different performance functions, the problem (e.g., addressed in an early study by Balch and Arkin, 1998) typically aims to optimize multi-robot trajectories by controlling leader-follower trajectories, specifying a reference point and defining a virtual structure. Egerstedt and Hu (2001) presented a strategy on solving path following problem based on multi-agent formation specifying virtual leader tracks as the reference trajectory, and avoiding obstacles by following a reference path. Focusing on minimizing system cost with a user-defined global function for using in D* incremental search algorithm (Stentz, A., 1994), Guo and Parker (2002) proposed an optimal motion planning model based on searching path and velocity patterns with safety margins by using a multidimensional state approach, which covers system states such as start and goal positions, environmental aspects and communication with other robots.

In addition to optimizing the system performance, more inherently, the analysis on stability of the system and how to stabilize the system are also critical for controlling autonomous vehicles in traffic systems. Based on the given vehicle reference posture and velocities, Kanayama et al. (1990) proposed a stable tracking control rule for non-holonomic autonomous mobile robots to find the most reasonable velocities, and Lyapunov function was adopted to prove the stability of the proposed rule. De Wit and Sordalen (1992) analyzed the exponential stabilization of two-degree-of-freedom mobile robots with non-holonomic constraints by a specific class of piecewise continuous controllers. Recently, Miao and Wang (2015) provided a time-dependent adaptive control scheme at the torque level to address the stabilization issue and tracking problem for unicycle mobile robots with unknown dynamic parameters depending on the instantaneous and past information of the reference velocities.

1.3 Motivation and challenges

While previous studies in the areas of vehicle motion planning have made important contributions in various aspects, it is still critically important to develop mathematically rigorous optimization models and computationally tractable algorithms to (1) consider the dynamic effect of vehicle interactions and also (2) reach the full potential of many system-level performance measures such as throughput, capacity, stability and safety. Along this line, this paper aims to address the following theoretical research questions.

1) How to adapt the current car-following models to model traffic interactions of automated vehicles based on available connectivity and automated functions, and in particular the dynamic process of tight platoon formation and system-level control?
2) How to develop a theoretically rigorous optimization model (e.g., in the form of mixed integer programming models) which could be solvable using standard optimization software such as CPLEX? Desirable multi-vehicle trajectory optimization models should be able to not only satisfy critical operational constraints such as obstacle avoidance, but also recognize the inherent nature of car following behavior to optimize platoon-level or system-level performance.
3) How to design on-line trajectory optimization algorithms to improve the performance of coupled AVs in a platoon, under complex traffic conditions with time-dependent capacity bottlenecks and obstacles of moving trajectories?

Since vehicle dynamics is nonlinear in nature, most existing AV controller designs involve sophisticated nonlinear feedback loops through time-continuous car following models. To provide tractable mathematical models for both offline and on-line vehicle trajectory optimization, we reformulate Newell's simplified car-following model in a discretized high-resolution space-time lattice. As a result, we could approximate the time-continuous vehicle trajectory control problem first though a binary integer programming model, which enables a rich body of standard optimization algorithms such as branch and bound and column generations. To further develop a solid theoretical foundation for multi-vehicle optimal control and efficient on-line optimization processes, we develop a family of efficient DP algorithms to schedule the optimal trajectory for multiple vehicles in a platoon. In particular, a new control variable of time-dependent platoon-level reaction time is introduced in this study to reflect various degrees of vehicle-to-vehicle or vehicle-to-infrastructure communication connectivity. By adjusting the leading vehicle's speed and (location-dependent) platoon-level reaction time at each time step, the proposed DP algorithms could effectively control the complete set of trajectories in a platoon, along traffic backward propagation waves. This parsimonious multi-vehicle state representation sheds new light on forming tight and adaptive vehicle platoons at a capacity bottleneck. As a reduced reaction time in a platoon is associated with potentially negative safety impact due to possible communication delay and failure, we also extend a model by Przybyla et al. (2015) to analytically evaluate the situational risk associated with communication delay. By dynamically configuring vehicle reaction times that could form different slopes of backward waves, we

hope a platoon with adaptive reaction times could better balance the goals of capacity throughput maximization and risk minimization, under complex driving and communication support conditions.

The rest of this paper is organized as follows: In section 2, we describe how to adapt the traffic flow theories developed by Newell (2002) and related kinematic wave model to characterize the AVs' dynamic trajectories. In section 3, we will develop an integer programming model to optimize the vehicle trajectories subject to minimal safe driving distances between cars, as well as different entrance and exit boundary conditions for using this formulation. In section 4, a sequence of dynamic programming based solution algorithms are further developed for different scenarios to optimize the vehicle speed profiles as well as to predict the optimized vehicle's impact on the following AVs. Finally, we demonstrate the potential of optimal trajectory control for both a single AV and multiple AVs through numerical analysis in section 5.

2. Modeling simplified car-following behavior

2.1. Simplified car-following behavior for AV

The notation used in this section is listed below.

L: length of vehicle (e.g., 20 feet or 4 meters)
d_n: minimum distance between the front of the leading car and the front of following car
d_0: the minimum safe rear-to-end distance after an emergency braking event
v_f: maximum or free-flow driving speed
$x_n(t)$ and $x_{n-1}(t)$: the position of following and lead vehicles, respectively, at a given time t
S_n: distance headway between the positions of leading and following vehicles
v_n: speed of the vehicle n
a_n: the deceleration rate of vehicle n
$I_n(t)$: time headway between n^{th} and $(n-1)^{th}$ vehicles
τ_{PR}: perception-response time (PRT)
τ_n: slope in a linear spacing-speed function
τ_B: redundant time buffer used in linear car following model for autonomous vehicles
k_{jam}: jam density
w_b: backward wave speed.

To clearly examine the perception-reaction and collision-avoidance mechanism for AVs, we first briefly review the related first-order car following models. Focusing on the time dimension in the car following behavior, Forbes' model (1958, 1963) considers two major elements: (i) the reaction time (e.g., 1.5 seconds) needed for human drivers to perceive the need to decelerate and apply the brakes; and (ii) the time duration for the following vehicle traversing its length (to avoid collision). Eq. (1) shows the equivalent distance headway.

$$d_n = 1.5v_n + L \tag{1}$$

In our research, using the human-driver car following behavior as the baseline, we are interested in how to adopt a linear car following model to approximate the time-continuous AV trajectories while maintaining the minimum safe driving distances. In the original classical paper by Newell (2003), he derived the linear car following model as an approximation of high-order trajectories (through the mean-value theorem), while our focuses below are on how the underlying AV collision-avoidance behavior leads to space-time relationship between a pair of leading and following vehicles, as the collision-avoidance constraint between a pair of vehicles is a building block of the proposed optimization models.

First, we need to compute the minimum safety distance S_n based on the driving speed of both cars (namely v_{n-1} and v_n) before the emergency braking. The process of one leading vehicle $n-1$ and one following vehicle n under emergency braking condition is illustrated in Fig. 1.

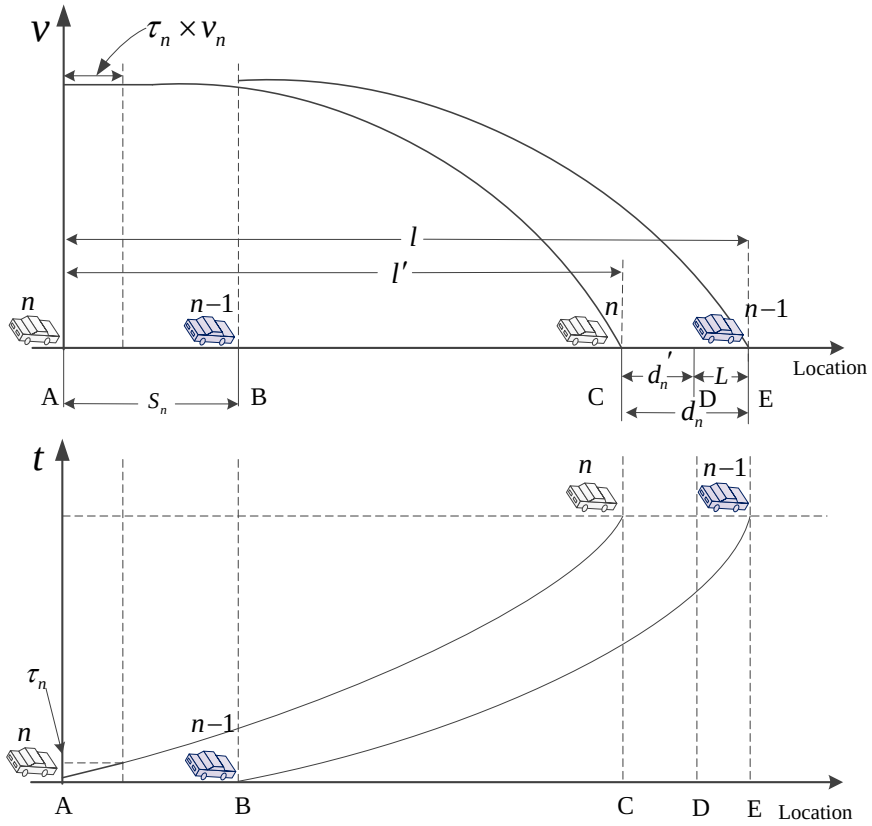

Fig. 1. The process of car-following behavior change.

Given the deceleration rates a_{n-1} and a_n, it is easy to derive the braking distances $l = S_n + \frac{v_{n-1}^2}{2a_{n-1}}$ and $l' = v_n \times \tau_n + \frac{v_n^2}{2a_n}$ and then establish Eq. (2) between S_n and d_n.

$$d_n = l - l' = S_n + \frac{v_{n-1}^2}{2a_{n-1}} - v_n \times \tau_n - \frac{v_n^2}{2a_n} \tag{2}$$

which can be rewritten as

$$d_n = S_n - v_n \times \tau_n + \frac{v_{n-1}^2}{2a_{n-1}} - \frac{v_n^2}{2a_n} \tag{3}$$

Since the following vehicle is tightly following the lead vehicle, we can assume $a_{n-1} = a_n$ and $v_{n-1} = v_n$ for the same or similar type of vehicles at the stable condition. In other words, our derivation focuses more on the stable states before and after the speed changes (state transition), so one can obtain Eq.(4).

$$S_n = \tau_n v_n + d_n \tag{4}$$

Eq. (4) is consistent with Newell's simplified car-following model that distance headway S_n changes linearly with speed v_n, where τ_n and d_n are independent of its vehicle speed v_n . The relation between spacing S_n and velocity v_n and the simplified car-following trajectory is shown in Fig.2.

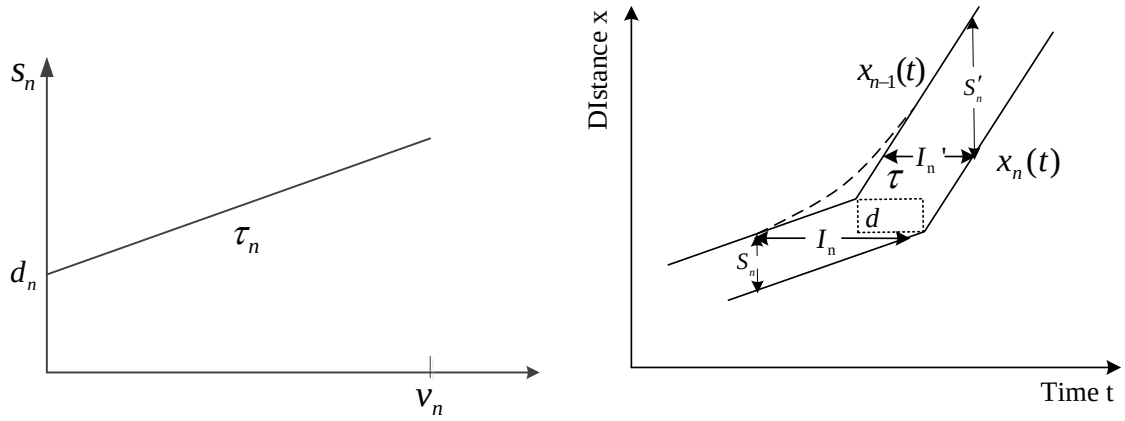

Fig. 2 Relation between spacing and velocity and piecewise linear approximation to vehicle trajectories with a speed change (adapted from Newell 2002)

Now we discuss possible values of perception and reaction time parameter τ_n under different cases.

(I) If the lead car is human operated (but possibly connected) and the following one is an automated car, τ_n should include a detection delay (about 0.3s) and emergency braking delay (about 0.4s), as shown by Ioannou et al (1994).

(II) If both vehicles are AVs and their driving speed information is completely shared in real time, τ_n can be significantly small as 0. This implies that $S_n = d_n$. This case applies to the AVs among an AV platoon.

To reduce the unexpected secondary accident impact, and to ensure the overall system reliability and stability, in the AHS designed by Varaiya (1993) and Bose and loannou (2003), an extra distance buffer $v_n \times \tau_B$ is given as shown in Eq. (5).

$$S_n = v_n \times \tau_{PR} + v_n \times \tau_B + d_n \tag{5}$$

where $\tau_{PR} + \tau_B$ in Eq. (5) is the desired time headway of autonomous vehicles, defined as the time taken to cover the distance $S_n - d_n$. Within a speed-spacing relationship described in Eq. (4), a unified formula for the slope parameter τ_n can be represented as $\tau_n = \tau_P + \tau_R + \tau_B$, where τ_P and τ_R are the corresponding perception and reaction time and $T_{PR} = \tau_P + \tau_R$.

Table 1 further examines the differences of the above mentioned car-following models in both human operated and autonomous vehicles.

Table 1. Different interpretations of linear car following model $S_n = \tau_n \times v_n + d_n$ with sample settings

Model	Time Offset τ_n			Distance offset
	Perception time	Response time	Redundant time buffer	
Newell's Model (human operated cars)	1-1.3	0.4	Not defined	d_n
Automated and connected car model	Very small, related to communication delay	Very small, related to machine and vehicle processing time	τ_B	d_n

In this section, we are interested in deriving the corresponding macroscopic flow-speed or flow-density relationship based on the proposed microscopic AV driving behavior, like given τ_k and d_k. As shown in Fig. 2, based on Eq. (4), we can derive the time headway $I_n(t)$ between n^{th} and $(n-1)^{th}$ vehicles as shown in Eq. (6),

$$I_n = \frac{S_n}{v_n(t)} = \frac{\tau_n \times v_n(t) + d_n}{v_n(t)} = \tau_n + \frac{d_n}{v_n(t)} \tag{6}$$

So the general time headway can be as, $\bar{I} = \bar{\tau} + \frac{\bar{d}}{v}$, where $\bar{\tau} = \frac{1}{n}\sum_{k=1}^{n} \tau_k$ and $\bar{d} = \frac{1}{n}\sum_{k=1}^{n} d_k$

Since the flow rate q can be expressed as $q = \frac{1}{\bar{I}}$, the capacity (maximum flow rate) is derived when speed reaches the maximum speed, free-flow speed v_{max}.

$$q_{max} = 1/(\bar{\tau} + \frac{\bar{d}}{v_{max}}) \tag{7}$$

Where jam density $k_{jam} = \frac{1}{\bar{d}}$, and backwave speed

$$w_b = \frac{q_{max} - 0}{k_{jam} - k_c} = \frac{\bar{d}}{\bar{\tau}}. \tag{8}$$

Eqs. (7) and (8) have been shown as a critical bridge between Newell's microscopic car-following model and macroscopic flow-density fundamental triangle diagram, and many studies (e.g., Mahmassani, 2016) have used a similar form to quantify the capacity impact under a connected or automated vehicle environment under different driving conditions.

2.2. Model leader-follower behavior in multi-AV formation control with changeable reaction times

As shown in the right plot of Fig. 2, before the speed changes from v_1, one can show that, $s_n = \tau_n \times v_1 + d_n$. If the velocity changes to v_2 , similarly, it can obtain $s_n' = \tau_n \times v_2 + d_n$. Assuming that the following vehicle n is tightly following the lead vehicle $n-1$, it is obvious that $x_{n-1}(t) - x_n(t+\tau_n) = S_n - \tau_n \times v_1 = d_n$ and $x_{n-1}(t) - x_n(t+\tau_n) = S_n' - \tau_n \times v_2 = d_n$. Thus we can further derive the car-following constraints in the time and space dimension, before and after speed changes.

$$x_n(t+\tau_n) = x_{n-1}(t) - d_n \tag{9}$$

By considering both free-flow and car following mode, we can obtain an inequality constraint in Eq. (10) shown by Newell (2002) as shown in Fig. 3.

$$x_n(t+\tau_n) = \min\{x_n(t) + v_f \times \tau_n, x_{n-1}(t) - d_n\} \tag{10}$$

If we extend Eq. (10) to another following vehicle n + m recursively, one can easily derive

$$x_{n+m}(t + \sum_{i=n}^{n+m} \tau_i) = \min\{x_{n+m}(t) + v_f \times (\sum_{i=n}^{n+m} \tau_i), x_{n-1}(t) - \sum_{i=n}^{n+m} d_i\} \tag{11}$$

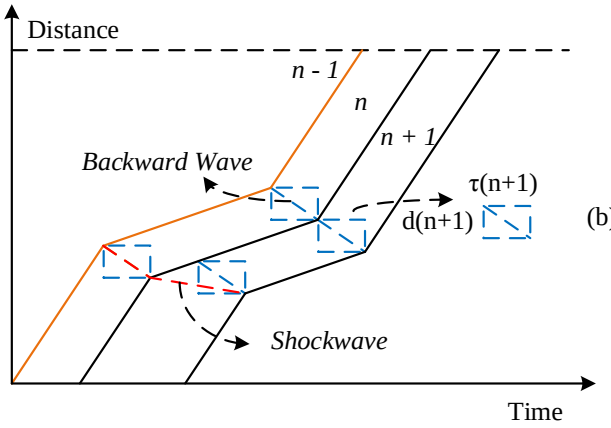

(a) Vehicles' trajectory based on simplified car following model

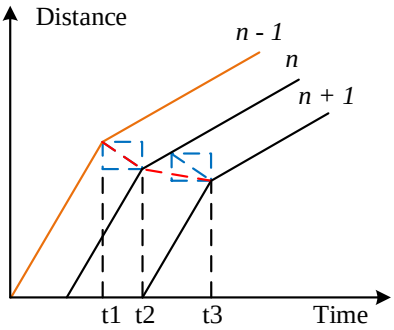

(b) Vehicles' trajectory from free flow speed to Congested speed

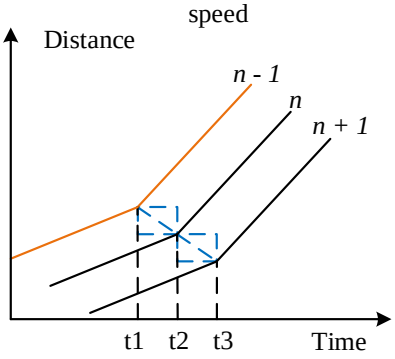

(c) Vehicles' trajectory from congested speed to free-flow speed

Fig. 3. Vehicle trajectories based on simplified car following model

Now, to better control the multi-robot trajectory, we consider a leader-follower formation control approach with dynamically changing reaction times, which is motivated by two reasons: (i) it is still a challenge to fully control each individual autonomous vehicle in a large scale, and (ii) a changeable reaction time (which is greater than the minimum reaction time) can reduce the collision risk, to some extent. The details will be discussed later.

Trajectories of a platoon consisting of 5 AVs are shown in Fig. 4(a) with constant reaction time and variable speed 30 mph to 60 mph. As shown in Eq. (6) or (7), capacity or time headway consumed by a set of vehicles, is dependent on two factors: reaction time and speed. By reducing or dynamically changing the reaction time during the journey of a multi-vehicle moving process, as illustrated in Fig. 4(b), we can increase the capacity throughput at the critical bottleneck as shown in Fig. 4(d) and Fig. 4(e) where the speed is 30 mph. All AVs in the platoon can pass the bottleneck without any splitting when the reaction time is 0 s in Fig. 4(d) and Fig. 4(e). To show the effectiveness of changing reaction times, possible trajectories of AVs with regular reaction time, $\tau_1 = 1.5\ s$, are plotted as green dashed lines at the critical bottleneck. As can be seen in Fig. 4(d) and Fig. 4(e), if the reaction time didn't change, not all AVs in the platoon could pass the bottleneck without splitting. That is, 2 vehicles in Fig. (4d) and Fig. (4e) are left behind the green time interval.

When we are able to adjust the variable reaction time between two optimization time steps, we need to carefully consider a special constraint to ensure the follower still moves forward as a result of two backward wave propagations. As shown in Fig. 4(b), after changing the reaction time, the new timestamp of the follower must be greater than the previous timestamp, which leads to Eq. (12).

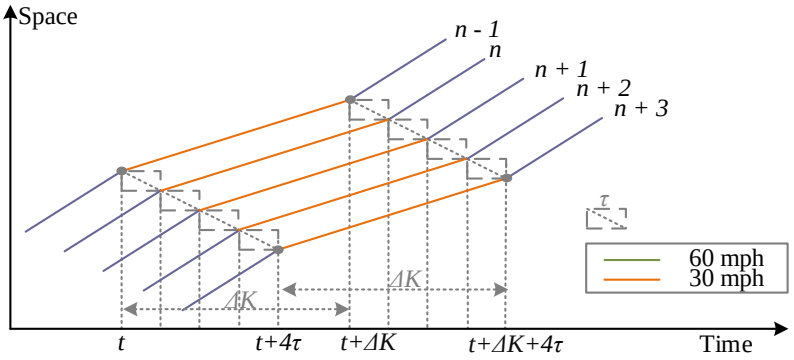

(a) Constant reaction time, speed is changing from 60 mph to 30 mph and from 30 mph to 60 mph

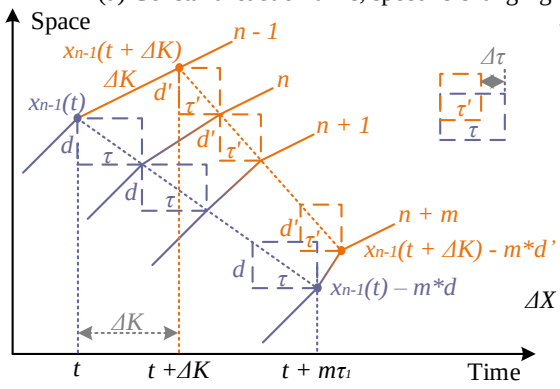

(b) Reaction time changing constraints

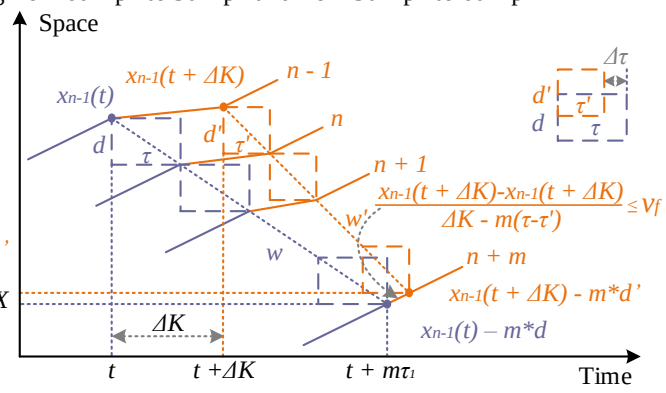

(c) Speed limit for transition process

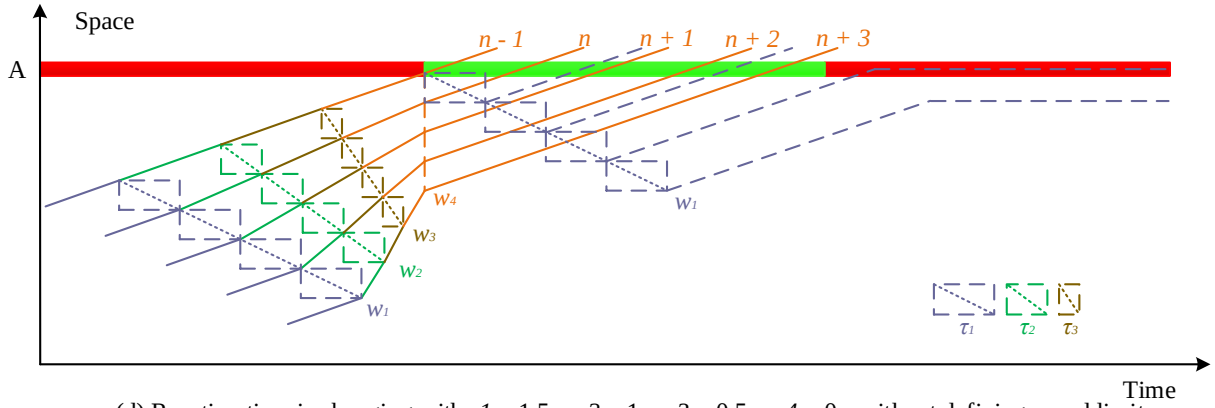

(d) Reaction time is changing with $\tau 1$ = 1.5 s, $\tau 2$ = 1 s, $\tau 3$ = 0.5 s, $\tau 4$ = 0 s without defining speed limit

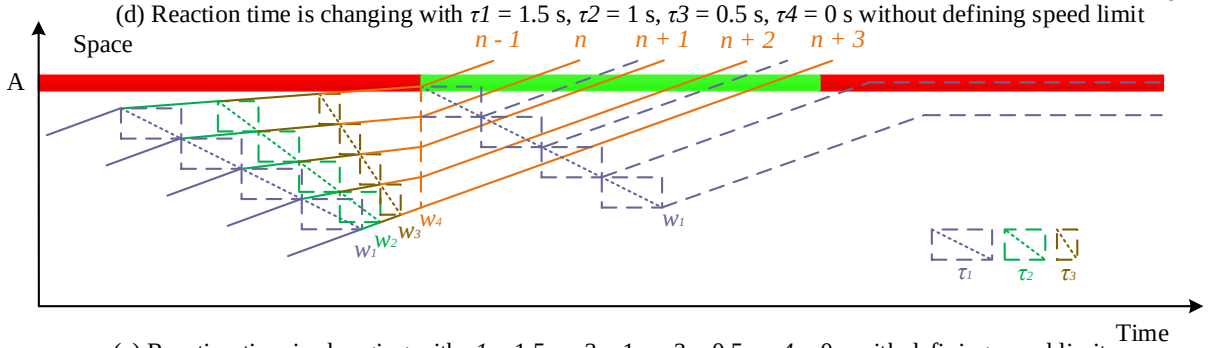

(e) Reaction time is changing with $\tau 1$ = 1.5 s, $\tau 2$ = 1 s, $\tau 3$ = 0.5 s, $\tau 4$ = 0 s with defining speed limit

Fig. 4. Vehicle trajectories with changing reaction time

$$t + \Delta K + m * \tau' > t + m * \tau \quad (12)$$

where ΔK is time difference between timestamps of reaction time change events, τ is the previous reaction time, τ' is current reduced reaction time. Assuming ΔK as 1 time interval, we can rewrite constraint (12) as $t + 1 + m * \tau' > t + m * \tau$, which leads to

$$(\tau - \tau') < \frac{1}{m} \quad (13)$$

That is, the magnitude of reaction time change $\Delta\tau$ must be less then $\frac{1}{m}$. After changing the reaction time, we need to ensure that the vehicle is not moving backward. That is, the new position of the followers must be larger than their previous position:

$$x_{n-1}(t + \Delta K) - m * d' \geq x_{n-1}(t) - m * d \quad (14)$$

where d and d' are the previous and current minimum distance between leading and following cars, respectively. For simplicity, if we assume d and d' have the same value, inequality (14) always holds.

It should be noted that in the transition process above, it is possible that the following vehicle(s) could have a short time period where the prevailing speed could temporally exceed the speed limit. For example, the lead vehicle is driving at the speed limit and the following vehicles need to catch up and form the platoon. This is the by-product of variable reaction times. To mitigate this issue, one could either reduce the speed of the lead vehicle to allow the following vehicles to catch up under the speed limit requirement, or expand the transition duration for variable reaction time so we have a smoother transition to reduce the possibility of temporally violating speed limit for the following cars.

To satisfy speed limits for all vehicles, it has to be define new constraint in the course of reaction time changing while vehicles are coupling. As shown in Fig. 4(c), while the last following vehicle keeps its speed, the leading vehicle should slow down. For the last vehicle: $\Delta X = (x_{n-1}(t + \Delta K) - m * d') - (x_{n-1}(t) - m * d)$. Since $d = d', \Delta X = x_{n-1}(t + \Delta K) - x_{n-1}(t)$. For the last vehicle: $\Delta T = (t + \Delta K + m * \tau') - (t + m * \tau)$, which leads to $\Delta t = \Delta K - m(\tau - \tau')$. Therefore, if the last vehicle cannot have a speed greater than speed limit, $\frac{\Delta X}{\Delta T} \leq v_f$. Thus we can further derive the speed limit constraint for changing reaction time.

$$\frac{x_{n-1}(t+\Delta K) - x_{n-1}(t)}{\Delta K - m(\tau - \tau')} \leq v_f \quad (15)$$

In general, a cooperative driving environment is expected to provide significant improvements for road safety and traffic flow efficiency (Kesting et al., 2010; Jia and Ngoduy, 2016a; Jia and Ngoduy, 2016b). Before presenting further analytical results, we now briefly review the related studies for measuring the impact of communication delay in different vehicular communication environments. Bai and Krishnan (2006) analyzed vehicle-to-vehicle (V2V) reliability in the application level, as a function of (i) distance headways between successive following vehicles and (ii) tolerance time window. According to their experimental results based on different distance headway from 25 m up to 400 m, packet delivery ratio, a common metric in the literature, is changing between 93% and 58%, respectively. Many studies, such as Xu et al. (2014), focused on quantitative characterization of the communication latency in a platoon, dependent on communication structures and content as well as communication standards. For instance, it has been shown that communication delay can reach up to 1.5 s within the IEEE 802.11p standard, and a failed transmission of vehicle braking events could have a ripple effect on all following vehicles. More recently, the concept of 5G network has been widely discussed for supporting autonomous vehicles to provide better data capacity, scalability of network, ultra-low latency and V2V connectivity (Kreutz et al.,

2015; Akyildiz et al., 2016; Intel, 2017). For example, Cheng et al. (2017) proposed a 5G-enabled cooperative intelligent vehicular (5GenCIV) framework to provide secure autonomous driving by enabling ultra-low latency typically requiring a time delay in the scale of microseconds, which could enable higher speed and lower space in the CAV environment discussed in our paper.

With changeable reaction time, we not only need to precisely compute the benefit of increased capacity, but also estimate the associated risk due to reduced reaction time threshold, as shown in the probability density function (PDF) of communication delay in Fig. 5(a). τ_n is a team-based reaction time threshold agreed upon by each vehicle in the platoon. τ_x is the extra communication delay (due to transmission error of data) beyond τ_n, and τ^a is the actual combined time delay as the summation of τ_n and τ_x. The magnitude of τ_x depends on the specific communication system used. As Fig. 5(a) shows, τ_x is greater under a standard communication system (e.g. DSRC) than under enhanced communication system (e.g. 5G). In a perfect car following behavior, the following vehicle should start to slow down at time $t + \tau_n$, , and starts emergency braking at time $t + \tau^a$. For a given extra delay τ_x, the braking time is $\Delta t_{TC} = \frac{v_n - v_{n-1}}{a_n}$ and the braking distance is $\Delta x_{TC} = \frac{v_n^2 - v_{n-1}^2}{2a_n}$. , as illustrated by the space-time diagram shown in Fig. 5(b).

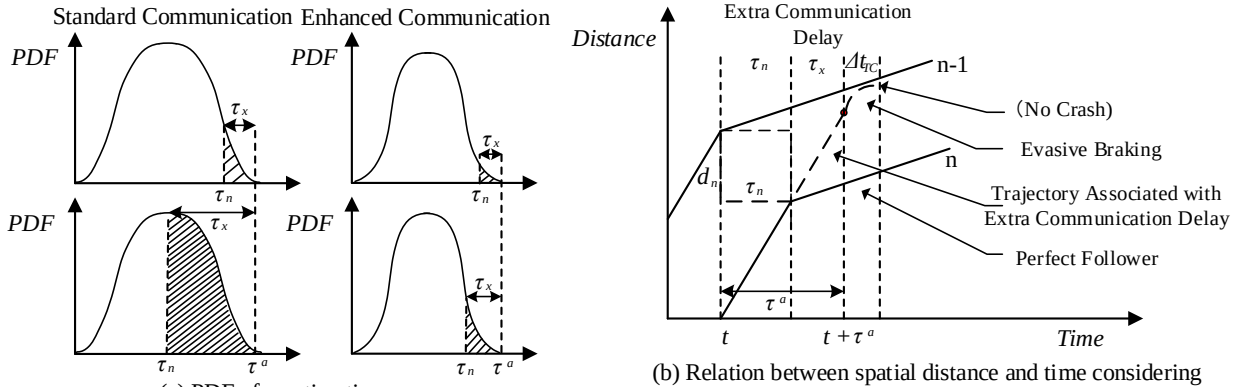

(a) PDF of reaction times

(b) Relation between spatial distance and time considering response time lag

Fig. 5. Probability density function (PDF) of communication delay and its impact on driving risk (adapted from Przybyla et al. (2015).

In order to guarantee the leading and following vehicles (X_{n-1}^a and X_n^a) do not collide, the position relationship between them at time ($t + \tau^a + \Delta t_{TC}$) should meet the following inequality constraint.

$$X_{n-1}^a(t + \tau^a + \Delta t_{TC}) \geq X_n^a(t + \tau^a + \Delta t_{TC}) + L \quad (16)$$

Following the derivation step by Przybyla et al., (2015) for distracted driving, at time ($t + \tau^a + \Delta t_{TC}$), the position of the leading and following vehicle could be represented as

$$X_{n-1}^a(t + \tau^a + \Delta t_{TC}) = v_{n-1} \times (\tau^a + \Delta t_{TC}) + X_{n-1}^a(t) \quad (17)$$

$$X_n^a(t + \tau^a + \Delta t_{TC}) = X_{n-1}^a(t) - d_n - \tau_n * v_n + v_n \times \tau^a + \Delta x_{TC} \quad (18)$$

Using the Eqs. (16) and (17), the probability of success equals to

$$P_{s_n} = Prob(X_{n-1}^a(t + \tau^a + \Delta t_{TC}) > X_n^a(t + \tau^a + \Delta t_{TC})) \quad (19)$$

It should be noted that the probability of success depends on the distribution of actual communication delay τ^a, and the preset response time value τ_n for given speed and positions of two vehicles. The team-based risk probability for m vehicles in the platoon can be calculated as follows

$$R_c = 1 - \prod_{n=1}^{m} P_{s_n} \quad (20)$$

3 Binary integer programming formulation

3.1 Problem statement

To construct the binary integer programming model, without loss of generality, we only consider autonomous vehicles along a single-lane facility with a given communication system. As shown in Fig. 6 (a), there are two segments AB and BC, and each segment has a communication system, which provides the reaction time of those autonomous vehicles or backward wave speed in those segments. The corresponding time-discretized space-time network is built in Fig. 6 (b). At each time stamp along time horizon from 0 to *T*, one vehicle can travel in one of *K* (*K*=4) alternative speed values from 0 to its speed limit, which can be represented by travelling arcs and waiting arcs. The travel cost of each arc in the space-time network is defined as its travel time in advance. At each physical destination node, a corresponding virtual super-destination node is built at the big time T. The travel cost of arcs from the destination node to the virtual super node is 0. To avoid the obstacles such as the time period of traffic red signals, we can delete those travelling arcs which go through or depart at the signal red time at the signal location in the space-time network.

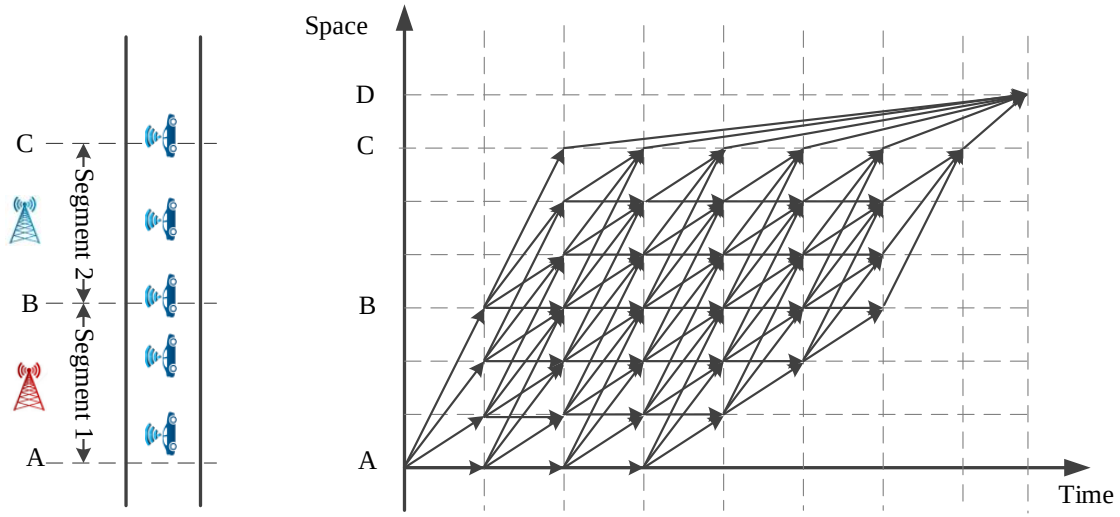

(a) Illustration of physical communication and traffic network

(b) corresponding extended space-time network

Fig. 6. Illustration of physical communication and traffic network and its space-time network

The relation between the lead vehicle and the following vehicle is displayed in Fig 7 (a) based on Newell's simplified car-following model, where the displacement of time and space establishes an incompatible area so that both vehicles cannot exist there simultaneously. The detail is further drawn in Fig 7 (b) when the reaction time and minimum spacing are 3-time interval and 3 space interval for the following vehicle, respectively. Fig 7 (c) shows the incompatible area with reduced displacement time from 3-time interval to 2-time interval. The set of incompatible points at each vertex can be enumerated based on the given reaction time or backward wave speed w in each segment with a built communication system. In short, our problem

aims to optimize all autonomous vehicles' trajectories to minimize the total system travel cost while satisfying Newell's simplified car-following constraints.

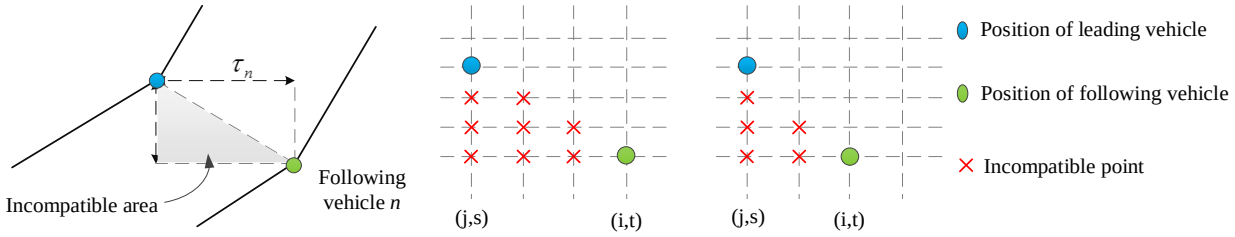

(a) space and time displacement in Newell's car-following model

(b) restricted area between lead vehicle and following vehicle

(c) restricted area between lead vehicle and following vehicle with reduced displacement time

Fig. 7. Illustration of restricted points based on Newell's car-following model

3.2 Mathematical programming formulation

Table 2. Notatin used for this section

Indices	Definition
i, j	Index of nodes, $i, j \in N$
(i, j)	Index of physical link between two adjacent nodes, $(i, j) \in L$
a	Index of agents/vehicles, $a \in A$
t, s	Index of time intervals in the space-time network
w	Index of communication time of autonomous vehicles
k	Index of segments with different communication time
$o(a)$	Index of origin node of agent a
$d(a)$	Index of destination node of agent a
Sets	
N	Set of nodes in the physical transportation network
L	Set of links in the physical transportation network
A	Set of agents
W	Set of communication time of self-driving cars
S	Set of segments
V	Set of vertices in the space-time network
E	Set of edges/arcs in the space-time network
Parameters	
DT^a	The departure time of agent a
AT^a	The assumed arrival time of agent a
$c_{i,j,t,s}$	Travel cost of traveling arc (i, j, t, s) in the space-time network
T	The time horizon in the space-time network
$\varphi_{(w,i,j,t,s)}$	$\varphi_{(w,i,j,t,s)} = 1$, if the vertex (j, s) visited by the following vehicle with reaction time w, the vertex (i, t) cannot be visited by its leading vehicle.
Variables	
$\theta_{i,t}^a$	Binary variable, indicator of vertex (i, t) visited by agent a
$x_{i,j,t,s}^a$	$= 1$, if Agent a is assigned on traveling/waiting arc (i, j, t, s) in the space-time network; $= 0$ otherwise

The objective function in Eq. (21) is to minimize the total generalized travel cost of all autonomous vehicles under centralized control. Eq. (22) is a standard vehicle-based flow balance constraint, similar to recent studies by Liu and Zhou (2016) and Lu et al. (2016). Eq. (23) defines whether or not vehicle a visits vertex (i, t) by $\theta_{i,t}^a$. Specifically, if $\theta_{i,t}^a = 1$, vehicle a visits vertex (i, t) and $\sum_{(j,s)} x_{i,j,t,s}^a = 1$, which

indicates that only one arc from vertex (i,t) is chosen. Otherwise, $\theta_{i,t}^{a}=0$, and no arcs from vertex (i,t) will be chosen by vehicle a. Inequality (24) represents the safe driving constraints of a pair of lead and following vehicles based on Newell's simplified car-following model. $\varphi_{(w,i,j,t,s)}$ is a parameter with value of 1 that defines the incompatible relation among vertexes (i,t) visited by the lead vehicle and the vertex (j,s) visited by the following vehicle under given reaction time/backward wave speed w at different road segments. As a result, our proposed model is a 0-1 integer linear programming model, which could be directly solved by standard optimization solvers, such as CPLEX.

Integer Programming Model:

Objective function:

$$\min \sum_a \sum_{(i,j,t,s)} x_{i,j,t,s}^{a} \times c_{i,j,t,s} \tag{21}$$

Subject to,

Vehicle-based flow balance constraint:

$$\sum_{i,t:(i,j,t,s)\in E} x_{i,j,t,s}^{a} - \sum_{i,t:(j,i,s,t)\in E} x_{j,i,s,t}^{a} = \begin{cases} -1 & j=o(a), s=DT^{a} \\ 1 & j=d(a), s=T \\ 0 & otherwise \end{cases}, \forall a \tag{22}$$

Indicator of vertex visited by vehicles:

$$\theta_{i,t}^{a} = \sum_{(j,s)} x_{i,j,t,s}^{a}, \forall (i,t), \forall a \tag{23}$$

Simplified car-following safety constraints:

$$\sum_{(i,t)} (\varphi_{(w,i,j,t,s)} \times \theta_{i,t}^{a}) + \theta_{j,s}^{a+1} \le 1, \forall (j,s) \in \varphi_{(w,i,j,t,s)}, \forall a \tag{24}$$

Binary variables: $x_{i,j,t,s}^{a} = \{0,1\}$;

As a remark, traffic boundary condition (closed or semi-open) is an important input for autonomous vehicle trajectory control/optimization. Our proposed model can handle not only the closed boundary condition in the space-time network but also the semi-open boundary condition through building a virtual super-destination node with the objective of travel time, fuel consumption, emissions, etc.

Fig. 8 illustrates in three dimensions (reaction time, space, and time) how reducing reaction times in follower vehicles increases capacity throughput at signalized intersections. The trajectories of the lead vehicle and four following vehicles are analyzed along a three-segment roadway with two traffic signals under three free flow speeds at different segments and four reaction times. Four different colors representing four changing reaction times (green for 1.5 s, blue for 1.0 s, brown for 0.5 s, and orange for 0 s).

In order to achieve a tightly coupled platoon with zero or closer-to-zero reaction time, as shown at intersections in Fig.8, this requires a future generation of communication standard higher than 5G with maximum service rate (MSR) of 4114 vehicles per hour per lane (vphpl) at intersection 1 and 6171 vphpl at intersection 2 for speeds of 30 km/h and 45 km/h, respectively. For a reaction time of 1.5 s, with the MSR of 1728 vphpl and 1516 vphpl for speeds of 45 km/h and 30 km/h, respectively, dedicated short range communication (DSRC) seems to be sufficient based on our very simplified analysis. More importantly, Fig. 8 aims to shed some lights to another important research problem, namely how to optimize vehicle/platoon approaches to signals considering this potential automated vehicle condition.

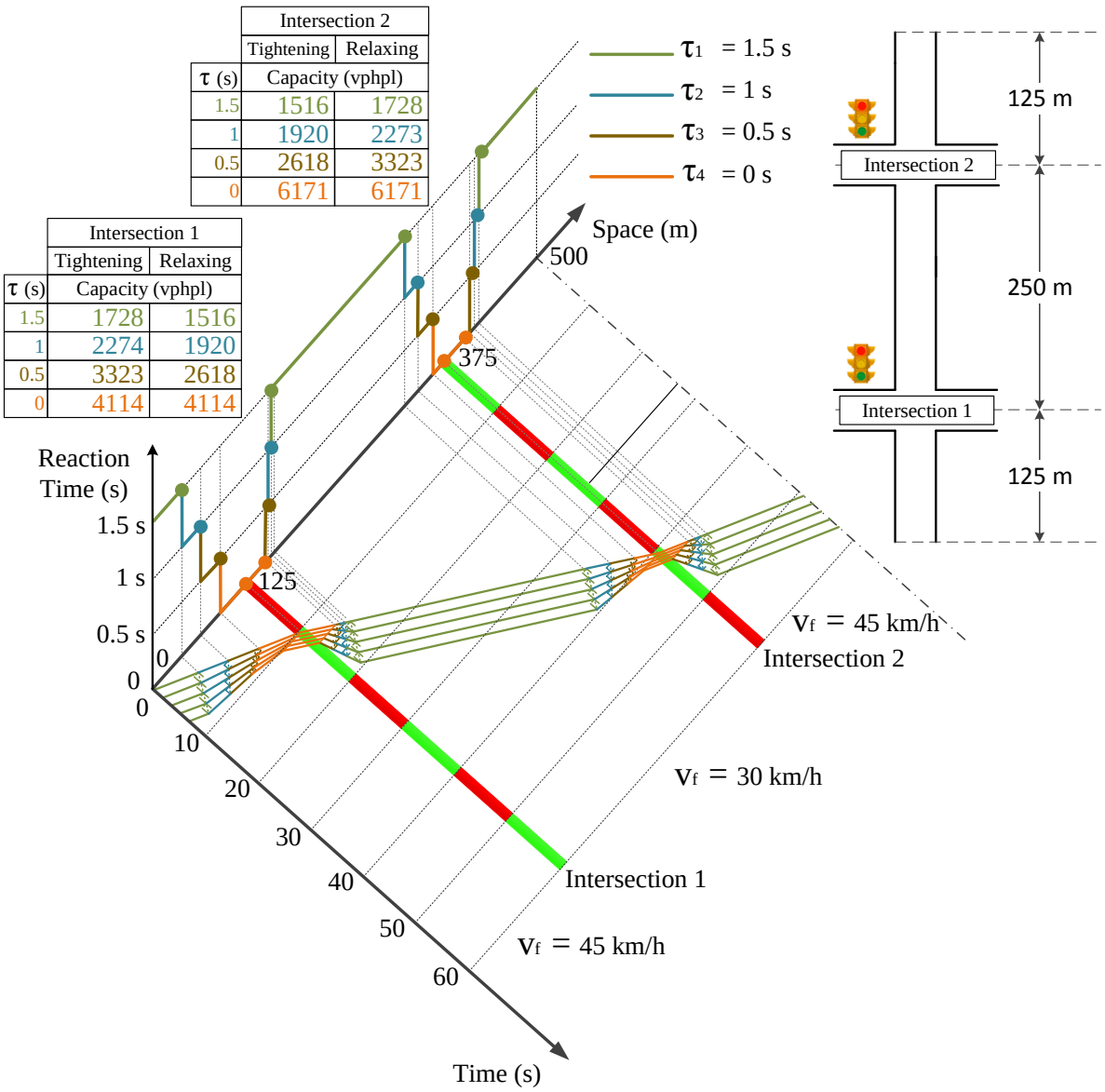

Fig. 8. 3D illustration of trajectories of AVs' and reaction time changing at the critical bottlenecks

The question for the collaborative vehicle driving is how the transition is carried out to maximize the throughput or capacity utilization, while balancing the risk associated with different reaction times.

As shown in Fig. (8) we can define a multi-dimensional arc variable as;

$x^a_{i,j,t,t',\tau,\tau'}$ = 1, if Agent a is assigned on traveling/waiting arc (i,j,t,t',τ,τ') in the space-time-reaction time network for using reaction time τ at time t, and using τ' at time t'

Subject to,

Vehicle-based flow balance constraint:

$$\sum_{i,t,\tau:(i,j,t,t',\tau,\tau')\in E} x^a_{i,j,t,t',\tau,\tau'} - \sum_{i,t,\tau:(j,i,t',t,\tau',\tau)\in E} x^a_{j,i,t',t,\tau',\tau} = \begin{cases} -1 & j = o(a), t' = DT^a, \tau' = \tau(0) \\ 1 & j = d(a), t' = T, \tau' = \tau(T) \\ 0 & otherwise \end{cases}, \forall a \quad (25)$$

In this extended formation, the indicator of a vertex visited by vehicles can be represented as

$$\theta^a_{i,t,\tau} = \sum_{(j,t',\tau')} x^a_{i,j,t,t',\tau,\tau'}, \forall(i,t,\tau), \forall a \quad (26)$$

One can still use the simplified car-following safety constraint (24) to ensure the 3D safety headway. Eq. (26) defines whether or not vehicle a visits 3D vertex (i,t,τ). Explicitly, when $\theta^a_{i,t,\tau} = 1$, vehicle a visits vertex (i,t,τ) and $\sum_{(j,t',\tau')} x^a_{i,j,t,t',\tau,\tau'} = 1$, which means that only one arc from vertex (i,t,τ) is selected. Otherwise, $\theta^a_{i,t,\tau} = 0$, and no arcs from vertex (i,t,τ) could be selected by vehicle a. Again, we need to impose τ transition constraints to ensure vehicles are moving forward, as shown in Fig. 4(b) and Eqs. (13) and (14). For example, the magnitude of the reaction time change $(\tau - \tau')$ must be less than $\frac{1}{m}$, where m is the size of a platoon.

As a remark, by enabling this variable reaction time process, we in fact aim to find an alternative method to indirectly implement the speed and trajectory control for multiple vehicles that form the platoon dynamically meanwhile considering tradeoff between safety and efficiency due to the possible communication delay. Specifically, we should note that the proposed model does assume the reaction time is controllable and its minimum reaction requirement is determined by the communication environment or the nature of the communication facilities. What is more, the result of controllable reaction time on following vehicles is our desired speed change or trajectory control for platoon formation under acceptable collision risks. In some cases, permitting the reaction time equal to 0 may cause traffic safety issue, while our examples could be easily re-implemented using a more realistic but small value like 0.1s or 0.5 s.

4. Dynamic programming for multiple vehicle trajectory optimization with changeable reaction times in a platoon

4.1 Different models and control variables

As shown in the extended form of Newell's car following model with multiple following vehicles in Eq. (11), one can control the lead vehicle to implicitly control all following autonomous vehicles. Overall, it is computationally involving to solve the proposed integer program using Eq. (23). To enable the real-time platoon formation and control, we transform the vehicle control model as a dynamic programming problem, which serves as a foundation for many vehicular movement controllers.

There are different levels of longitude vehicle trajectory control problems (with simplified car following model), as shown in Fig. 9. Table 2 lists all basic elements of dynamic programming for single vehicle trajectory control (mode 1) and two coupled vehicle trajectory control (mode 1+1), 1 leader controlling tightly coupled followers (mode 1+m), and 1 leader controlling tightly coupled followers with variable backwave speed w, (mode 1+m (w)).

Table 2. Description of different modes

No.	Mode	Description	Control Variable
(1)	1	One single optimized autonomous vehicle	Single vehicle trajectory
(2)	1 + 1	Two jointly optimized autonomous vehicles (the second vehicle is not necessary at a following mode)	Trajectories of leader and follower
(3)	1 + m	One optimized lead AV and m following vehicles with fixed reaction time	Trajectory of leader
(4)	1 + m(w)	One optimized lead AV and m following vehicles with variable reaction time	Trajectory of leader and (variable) platoon-level reaction time along backward wave line

In Fig. 9, the discretized time unit is one-time interval, and the discretized space unit is also defined on the basis of feasible vehicle speeds, which have three alternatives from 0 to the maximum speed limit for constraint (10). Assume that the optimized vehicle trajectory has been found through dynamic programming as shown in Fig. 9. The green trajectory is for the lead vehicle and the orange trajectory is for following vehicles. The dashed lines are the backward wave for the tight car following condition. The backward wave speed is equal to d/τ based on equation (8). For satisfying constraint (23), the solid red trajectory represents the safety boundary of the lead vehicle that all following vehicles cannot enter in Fig. 9(b).

Fig. 9(a) shows the possible trajectory of a single optimized autonomous vehicle from point A to point B. This trajectory is used as the leader trajectory for the other trajectory control modes in Fig. 9(b), (c), and (d). In Fig. 9(b) possible trajectories between the lead and the following vehicles are analyzed. The following vehicle starts with free flow speed until it reaches the lead vehicle safety boundary. At that point, the following vehicle adjusts its speed to that of the lead vehicle according to constraint (10). Fig. 9(c) depicts the trajectories of the optimized leading and multiple following vehicles with fixed reaction time where the leader is controlling the tightly coupled followers. The following vehicles in the platoon travel with the same speed as the leader. However, in the case of the optimized lead AV and multiple tightly coupled following vehicles with variable reaction time, as shown in Fig. 9(d), the trajectories of the following vehicles in the platoon vary according to the changing reaction times, according to a given objective function to optimize.

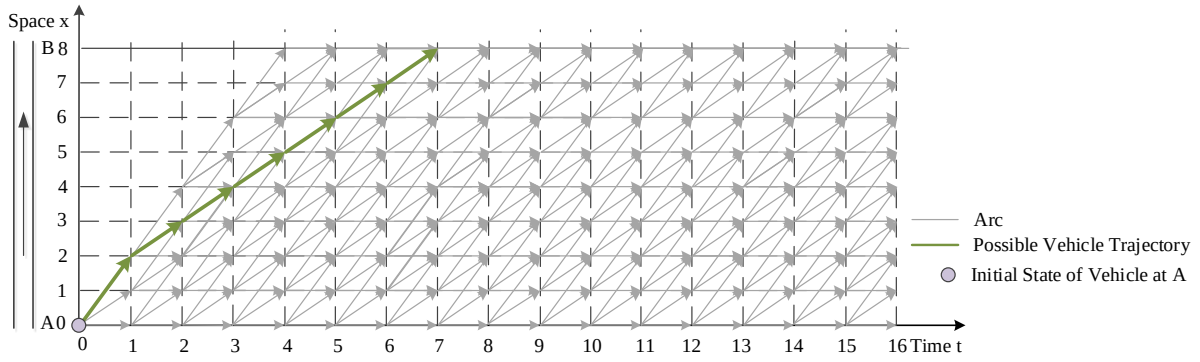

a) Discretized space-time network for vehicle trajectory optimization for (1)

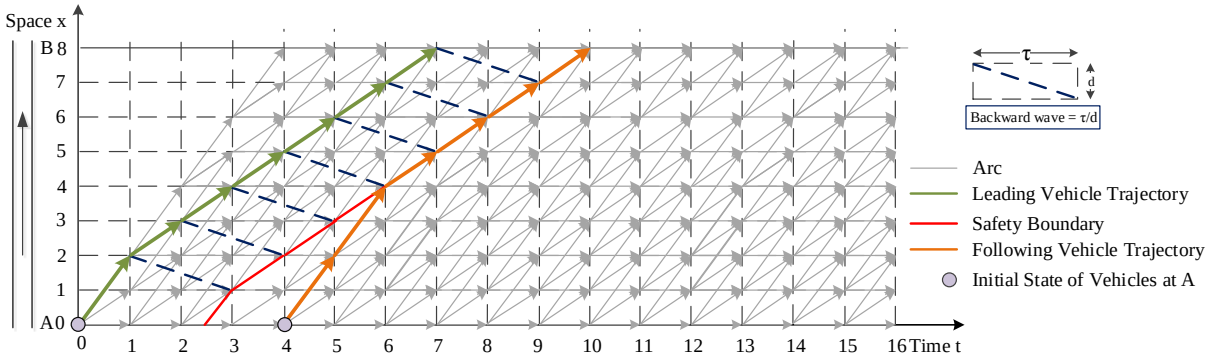

b) Discretized space-time network for vehicle trajectory optimization for (1+1)

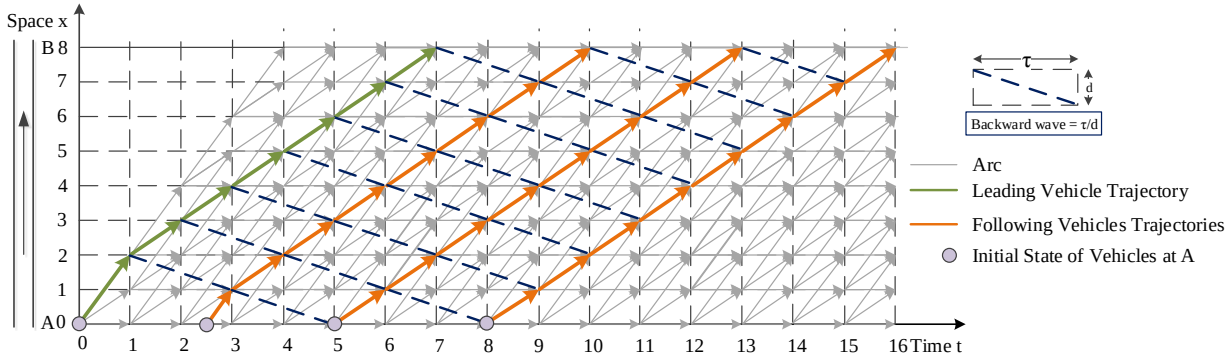

c) Discretized space-time network for vehicle trajectory optimization for (1+m)

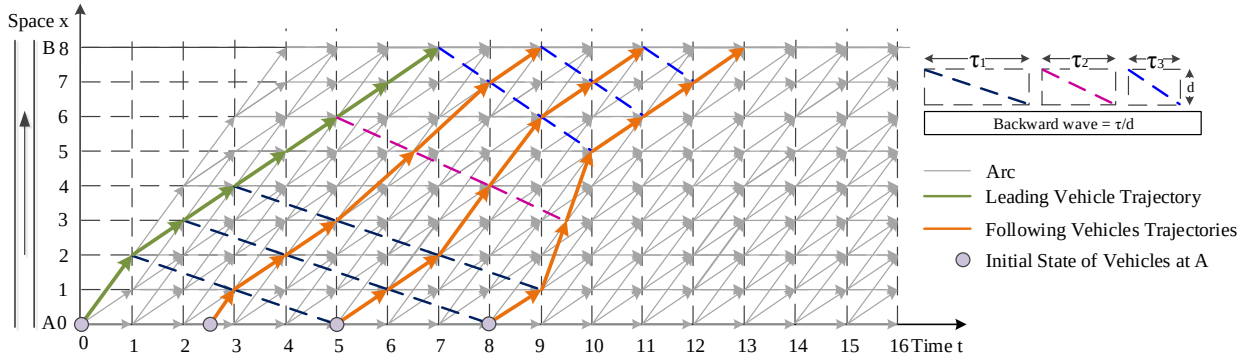

d) Discretized space-time network for vehicle trajectory optimization for (1+m(w))

Fig. 9. Discretized space-time network for vehicle trajectory optimization for all modes

4.2 Formulation and Optimality Conditions in Dynamic Programming for Coupled Vehicles

From the control point of view, it seems to be straightforward to control vehicle' speed and deceleration individually, but it is very complex and challenging to optimize all vehicles' trajectories independently. In our opinion, it is beneficial to first take a platoon-based approach for optimizing and synchronizing the same variable reaction time of m autonomous vehicles, depending on the available vehicle to vehicle communication capabilities, and then accordingly use this group of (optimized) reference trajectories to further apply vehicle speed and acceleration control at an individual level.

The dynamic programming proposed for the 4 modes in Table 3 is analyzed in Table 3.

Table 3. All elements of dynamic programming for all optimization types

No.	Elements	Single vehicle (mode (1))	Two vehicles (mode(1+1))	Multiple vehicles with fixed displacement time (mode (1 + m))	Multiple vehicles with variable displacement time (mode(1+m(w)))
(1)	Stage	$0,1,..,T$	$0,1,..,T$	$0,1,..,T$	$0,1,..,T$
(2)	State	$S=[x_1(t)]$ Location	$S=[x_1(t),x_2(t+\tau)]$ Location of leader, location of follower	$S=[x_1(t)]$ Location of leader, derived locations of followers 2, …, m	$S=[x_1(t),\tau(t)]$ Location of leader, derived locations of followers 2, …, m, reaction time τ for the platoon
(3)	Policy control/ decision variables	$v_1(t),(i.e.\,x_1(t+1)-x_1(t)$	$v_1(t),v_2(t+\tau)$	$v_1(t),v_m(t+\tau*m)$	$v_1(t),v_m(t+\tau(t)*m)$, reaction time $\tau(t)$
(4)	Vehicle location updating	$x_1(t+1)=x_1(t)+v_1(t)$	$x_1(t+1)=x_1(t)+v_1(t)$; $x_2(t+\tau+1)=min\{x_2(t+\tau)+v_2(t),x_1(t+1)-d_2\}$	$x_1(t+1)=x_1(t)+v_1(t)$; $x_m(t+\tau*m+1)=min\{x_m(t+\tau*m)+v_m(t),x_1(t+1)-d_m*m\}$	$x_1(t+1)=x_1(t)+v_1(t)$; $x_m(t+\tau(t)*m+1)=min\{x_m(t+\tau(t)*m)+v_m(t),x_1(t+1)-d_m*m\}$
(5)	Cost function for both control and derived variables:	$c[x_1(t),x_1(t+1)]$	$c[x_1(t),x_1(t+1),x_2(t+\tau),x_2(t+\tau+1)]$	Cumulative cost across all vehicles in a platoon $cc[x_1(t),x_1(t+1),x_2(t+\tau),x_2(t+\tau+1,\dots,x_m(t+\tau*m),x_m(t+1+\tau*m)]$	Cumulative cost across all vehicles in a platoon $cc[x_1(t),x_1(t+1),x_2(t+\tau(t)),x_2(t+\tau(t)+1,\dots,x_m(t+\tau(t)*m),x_m(t+1+\tau(t)*m)$
(6)	Value function for control variables	$L(t,x_1(t))$	$L(t,x_1(t),x_2(t+\tau))$	$L(t,x_1(t))$	$L(t,x_1(t),\tau(t))$

(1) Stage: based on the discretized time in the space-time network for mode (1), mode (1+1), mode (1+m) and in space-time-reaction time network for mode (1+m(w)), all modes can have the same stage from time 0 to time T;

(2) State: For mode (1), its state can be represented by location only as $S = [x_1(t)]$. For example, if the space-time network in Fig. 9 (a) is built for mode (1), the possible states are {0, 1, 2} when time is 1 depends on selected velocity.

For mode (1+1), since the two vehicles need to keep a safety spacing, we can represent the state as a safe-driving state vector with two dimensions as $S = [x_1(t), x_2(t+\tau)]$. If the space-time network in Fig. 9 (b) is used for illustrating mode (1+1), in order to satisfy constraint (10), the safety states are {0, 1, 2, 3, 4} at time 6.

Mode (1+m) considers the lead vehicle position as the state and then derives the locations for multiple following vehicles by using constant reaction time. Thus, we only have one independent state represented as an one-dimensional vector $S = [x_1(t)]$, shown in Fig. 9(c).

Mode (1+m(w)) adds variable reaction time into the state vector of mode (1+m), so the state in the platoon is represented as $S = [x_1(t), \tau(t)]$, shown in Fig. 9(d).

(3) Control: For mode (1), the control/ decision variable is the speed of optimized vehicle $v_1(t)$. There are two control/ decision variables in mode (1+1): the speed of the lead vehicle at time t, $v_1(t)$, and the speed of the following vehicle at a different time index $t+\tau, v_2(t+\tau)$. For mode (1+m), the control/ decision variable for the leading vehicle is $v_1(t)$. Mode (1+m(w)) considers two control variables $v_1(t)$ and $\tau(t)$, which further determine the remaining following vehicles' trajectories (as derived variables).

(4) Cost function of decisions used in optimality conditions: Mode (1) and mode (1+1) can be represented as $c[x_1(t), x_1(t+1)]$ and $c[x_1(t), x_1(t+1), x_2(t+\tau), x_2(t+\tau+1)]$, respectivly. The total system travel cost for multiple vehicles can be calculated by summing each vehicle's cost cumulatively in the platoon. The cumulative cost value in the case of platoon trajectory control for mode (1+m) and for mode (1+m(w)) can be represented as $cc[x_1(t), x_1(t+1), x_2(t+\tau), x_2(t+\tau+1), \dots, x_m(t+\tau*m), x_m(t+1+\tau*m)]$ and $cc[x_1(t), x_1(t+1), x_2(t+\tau(t)), x_2(t+\tau(t)+1), \dots, x_m(t+\tau(t)*m), x_m(t+1+\tau(t)*m)$, respectively.

If the capacity consumption is concerned for a tight car-following platoon, we can consider as maximum completion time as the cost of platoon, shown as the along time 0 to $(t+m*\tau)$ in Fig. 10. Please note that, the reaction time τ is a variable in this mode, thus the selection of τ would affect the boundary of the platoon. That is, a smaller reaction time can reduce the platoon footprint in the space-time diagram.

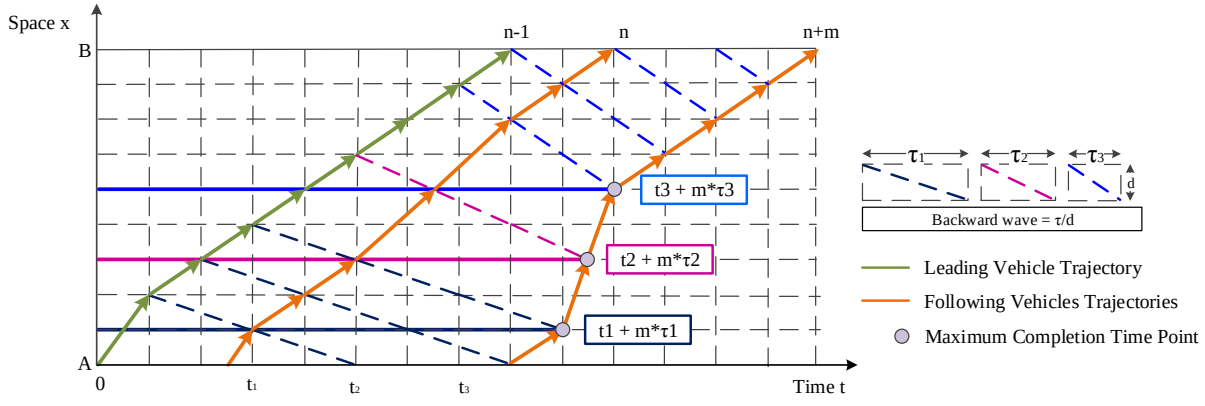

Fig. 10. Illustration of maximum completion time

(5) Value function: This is described as the cumulative value from stage 0 to the current stage. For both mode (1) and mode (1+m), it can be represented as $L(t, x_1(t))$. Since the two vehicles are controlling in mode(1+1), the label cost can be represented as $L(t, x_1(t), x_2(t+\tau))$as a 3-dimenstional vector. mode (1+m(w) also a 3-dimenstional label cost vector as $L(t, x_1(t), \tau(t))$, because of controlling multiple vehicle trajectories and reaction time.

The aforementioned problem contains two principle features: (1) it is in essence a discrete-time (e.g., every second) dynamic (i.e., time-dependent) system; (2) the total cost is additive in a sense that the generalized cost incurred at time k is accumulated over time. The system's state at time $t+1$ is only determined by the decisions made at t and its previous state at t. As a result, the optimal vehicle trajectories can be solved by using dynamic programming. Those algorithms mentioned in Table 3 will be stated in detail in section 4.3.

4.3 Dynamic programming algorithms

Mode ("1+m")

Denote $L(t, x_1(t))$ as the value function of state$(t, x_1(t), \ldots, x_m(t+\tau*m))$ at t, $t \in [0,T], x \in [0,D]$ and cc as the cumulative cost function from vehicle 1 to vehicle m in the platoon.

```
// initialization
L(t, x_1(t)) := +∞;
L(t, x_1(0)) := 0;
for t = 0 to T do //stage
  for x_1(t) = 0 to D do //state
    for x_1(t+1) = x_1(t) to x(t) + d^max do //control decision
      cc= c[x_1(t), x_1(t+1)]
      for m = 1 to M do
        x_m(t+τ*m+1) = min{(x_m(t=0) + v_f × (t + τ*m + 1), x_1(t) − Σ_{i=2}^{m} d_i} //(vehicle m's position
        cc = cc + c[x_m(t+τ*m), x_m(t+τ*m+1)]; // cost of decision
      endfor
      if x_1(t), x_1(t+1), x_2(t+τ), x_2(t+τ+1), …, x_m(t+τ*m), x_m(t+τ*m+1) are within feasible space-time
regions and L(t, x_1(t)) + cc < L(t+1, x_1(t+1))
      then  L(t+1, x_1(t+1)) = L(t, x_1(t)) + cc;
    endfor
  endfor;
endfor;
```

Mode ("1+m(w)")

Denote $L(t, x_1(t), \tau(t))$ as the value function of state $S = [x_1(t), x_m(t+\tau(t)*m)]$ at t, $t \in [0,T], x \in [0,D]$, $\tau \in [0, \bar{\tau}]$ and cc as the cumulative cost function from vehicle 1 to vehicle m in the platoon. Assume $\tau_U(d)$ as the maximum reaction time along d to D, $\tau_L(d)$ as the minimum reaction time supported by a selected communication technology along d to D, $\tau_{change}(t)$ as a binary variable along t to T satisfying the reaction time changing constraints in Eqs. (12), (13) and (14). By using the extended Newell's inequality constraint for multiple vehicles in Eq. 11 and control decision for leading vehicle as written $x_1(t+1) = x_1(t)$ to $x_1(t) + d^{max}$, the flow balance constraint in Eq.(24) is always ensured by controlling whether or not any vehicle visits 3D vertex (i, t, τ). In this proposed multi-vehicle control model, we can solve the semi-open boundary optimization problem, by only defining the initial position of vehicles, by building a time-space-reaction time network with the desired objective, such as emissions, fuel consumption, travel time etc.

The DP-based optimization algorithm is described as below:

// initialization
$L(t, x_1(t), \tau)) := +\infty$; // value of state $(x_1(t))$
$L(t = 0, x_1(0), \tau)) := 0$;
for $t = 0$ to T **do** // 1st loop: time stage
  for $x_1(t) = 0$ to D **do** //2nd loop: feasible space state
    for $x_1(t+1) = x_1(t)$ to $x_1(t) + d^{max}$ **do** //3rd loop: speed control decision
      for $\tau = \tau_L(x_1(t))\ to\ \tau_U(x_1(t))$ **do** //4th loop: reaction time levels
        for $\tau' = \max\left(\tau - \tau_{change}, \tau_L(x_1(t))\right) to \min(\tau + \tau_{change}, \tau_U(x_1(t)))$ **do** // 5th loop: reaction time change
          $cc = c[x_1(t), x_1(t+1)]$
          for $m = 1$ to M **do** //6th loop: number of vehicles in a platoon
            $x_m(t + \tau' * m + 1) = \min\{(x_m(t=0) + v_f \times (t + \tau' * m + 1), x_1(t) - \sum_{i=2}^{m} d_i\}$ // vehicle m's position
            $cc = cc + c[x_m(t + \tau * m), x_m(t + \tau' * m + 1)]$;// cost of decision
          endfor;
        if $x_1(t), x_1(t+1), x_2(t+\tau), x_2(t+\tau+1), \ldots, x_m(t+\tau*m), x_m(t+\tau*m+1)$ are within feasible space-time regions; and $L(t, \tau, x_1(t)) + cc < L(t+1, x_1(t+1), \tau')$
          then $L(t+1, x_1(t+1), \tau') = L(t, x_1(t), \tau) + cc$
        endfor;
      endfor;
    endfor;
  endfor;
endfor;

The corresponding DP algorithms for modes "1" and "1+1" can be found at Appendix A.

As stated in chapter 20 in the book by Jensen and Bard (2003), the dynamic programming approach has two different types of recursion relationships: backward recursion and forward recursion. As shown in our platoon trajectory optimization problem Mode "1+m", we use the following label cost updating functions (27) to implement the forward recursive equation (28):

If $L(t, x_1(t)) + cc < L(t+1, x_1(t+1))$ **then** $L(t+1, x_1(t+1)) = L(t, x_1(t)) + cc$; (27)

Forward recursive equation

$L(t+1, x_1(t+1)) = Min\{L(t, x_1(t)) + cc\}$ for time stage t=0, 1, …, T (28)

where cc is the cumulative cost across all vehicles in the platoon at time t ; and the vehicle location states are subject to the following two constraints.

$x_1(t+1) = x_1(t) + v_1(t)$;

$x_m(t + \tau * m + 1) = min\{x_m(t + \tau * m) + v_m(t), x_1(t+1) - d_m * m\}$

One can use a backward recovery procedure to identify the optimal path from the final state associated with the minimum label cost. A detailed discussion on the equivalent relationship between backward induction and forward induction can be also found in chapter 11 of the book by Bradley, Hax, and Magnanti (1977). In short, the procedure in our paper uses a forward recursive function from one time stage to a successor time stage, so the overall solution searching framework still follows a dynamic programming approach.

On the other hand, one could re-express the proposed forward DP model using a backward recursive search relationship and we do believe this backward approach is much closer to the original open-loop feedback control framework in standard DP. However, the classical backward (closed-loop) approach requires (i) a clear definition of the ending states and associated boundary conditions at time T and (ii) the initial state at time t=0 can be backward reachable from the defined ending states. In comparison, our proposed forward approach is more suitable for propagating the current initial states of the platoon into the (partially unknown) future states and one can select one of feasible ending states as the final optimal solution to back trace to the initial boundary.

It should be further remarked that, the model of 1+m(w) treats reaction time as discrete variables, so our problem indeed changes the feasible space compared with the original problem of controlling all vehicles with continuous reaction times. Under this feasible space, we only keep the best feasible solutions at each space-time-state vertex with the minimal label cost, and the other dominated solutions are pruned by the optimality conditions. If an enumeration algorithm is used (instead of our proposed DP algorithms), then one has to explore all possible paths from the beginning which might still contain many sub-optimal subpaths based on our proposed optimality criteria.

4.4 Improving computational complexity

As there are multiple loops in the proposed DP algorithm, we need to carefully examine its efficiency on a discretized network. For the first two loops with the time and space indexes, one can greatly reduce the space search range by considering the feasible prism of the vehicle trajectories, and a time geography based approach has been systematically discussed by Zhou et al. (2017). The 3rd loop is related to the maximum number of steps considered in the discretized grid, e.g., around 8-20 steps used in our experiment. The 4th loop is related to the number of reaction time levels, e.g., 4 levels for a maximum reaction time of 2 s. The 5th loop requires very limited efforts, as typically only very smooth changes (e.g., 0, 1, 2 steps) in reaction times are allowed. The last loop considers all the vehicles in a platoon, typically in a size of 2-4. Overall, even there are multiple nested loops in the proposed DP algorithm, many loops as associated with very small values and we could further intelligently reduce the search efforts by selecting the most likely and most promising state changes in order to avoid the curse of dimensionality.

Reducing search space in the discretized network is a potentially useful approach to improve the computational efficiency. For this purpose, we perform experiments to demonstrate how to reduce search space by selecting feasible space-time grid cells and maximum number of steps values for 2nd and 3rd loops. Fig. 11 shows three different search spaces: full search space without any optimization (a), reduced search space by assuming maximum speed limit and preferred latest arrival time as the space boundary (b), and reduced search space with optimized step size by additionally selecting desirable speed lower bound (c). Table 4 shows the resulting CPU running time by using a kind of traditional personal computer which has i7 CPU 2.4 GHz, 8 GB RAM, 256 GB SSD and optimizing steps for (b) and (c) in bold, for applying search space reduction before as (a) and after as (b) and (c), as 17.55 s, 13.24 s and 9.72 s, leading to an about 55% reduction in CPU time due to reduced search space.

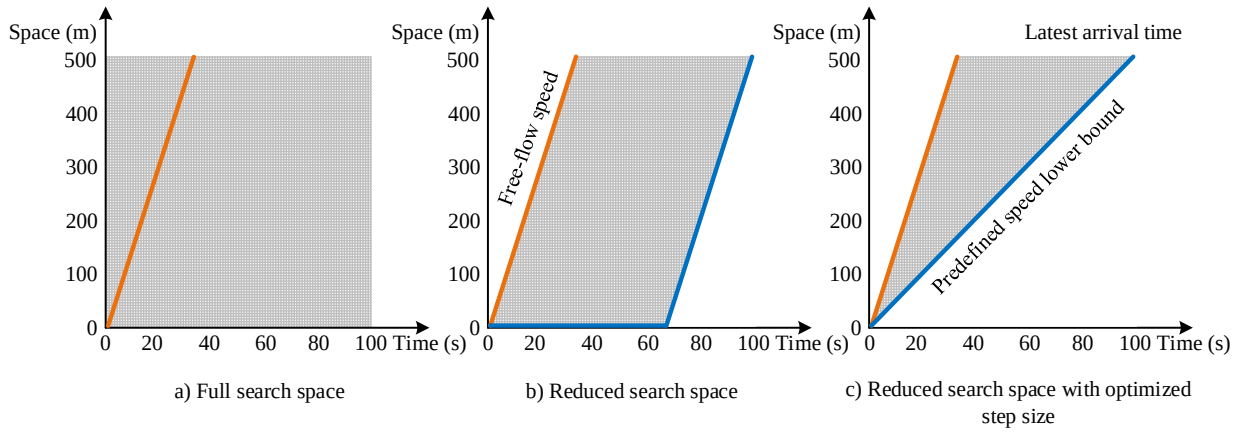

Fig. 11. Illustration of three different search space for mode 1+m(w)

Table 4. Processing time for three different cases

	a)	b)	c)
Time and space by using 0.5 s and 0.5 meters as simulation resolution, 1st and 2nd loops	$200*10^3$	$134*10^3$	$134*10^3$
Maximum number of the steps, 3rd loop	16	16	8
Reaction time levels, 4th loop	4	4	4
$\Delta\tau$, 5th loop	1	1	1
Vehicle count, 6th loop	5	5	5
Total	$6400*10^4$	$4288*10^4$	$2144*10^4$
CPU running time (s)	17.55	13.94	9.72

In addition, the possibility of considering the proposed trajectory control in a more complex condition, such as, the process of merging, is discussed in Appendix B.

5. Numerical Experiments

In this section, we perform experiments to demonstrate how to optimize vehicle trajectories by using dynamic programming and binary integer programming. Specifically, DP algorithms are performed for "1+m"(one lead automated vehicle control with considering the impacts to m human-driven following vehicles, which could be further organized as a platoon) and "1+m(w)" (one leading automated vehicle and m following automated vehicle's reaction time control), and The GAMS program (CPLEX) is used for our proposed integer programming models, which aim at modes "1+1" (or "1+1+1…") to control all autonomous vehicles individually for a small subset of vehicles due to the possible large number of integer variables. Modes "1+m" and "1+m(w)" solved by DP algorithms can be treated as special cases of integer programming models.

5.1. Platoon Analysis by using Mode "1 + m (w)"

Fig. 12 shows the layout of hypothetical environment, where the total length of the road segment is 1000 m and total time horizon is 150 s; the free flow speed is 60 kilometers per hour in segment 1 and segment 3, from origin to 250 meters and from 750 meters to 1000 meters, respectively. Segment 2 is a speed-reduction zone with the speed of 30 km/h from 250 meters to 750 meters. At 250 meters is a traffic signal where the red phase duration is 20 s and green is 15 s. In addition, there is a traffic signal at 750 meters where the red phase duration is 35 s and green is 20 s.

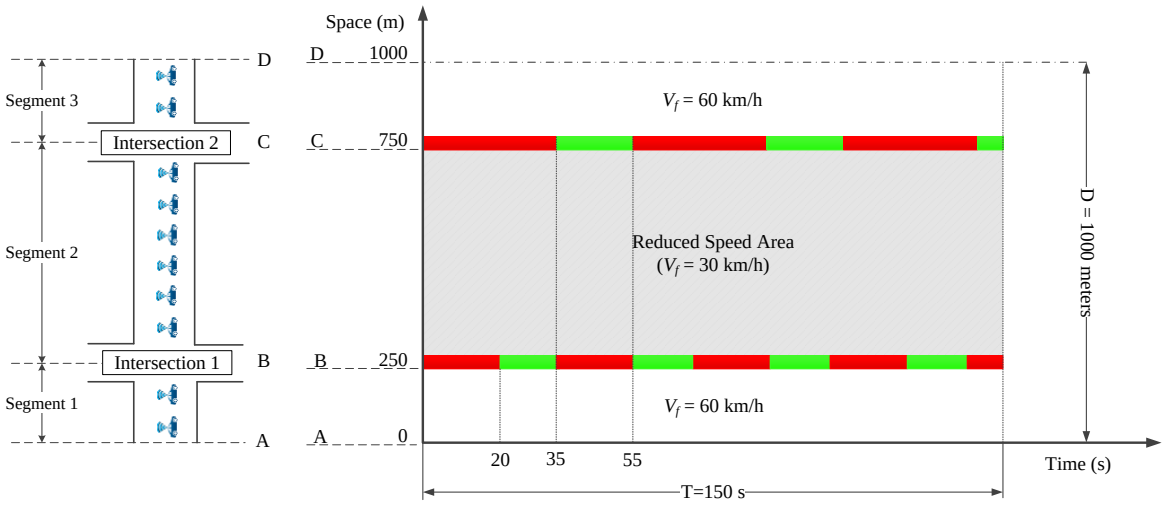

Figure 12: Layout of hypothetical road segment

The trajectory of the leader vehicle and reaction time in a platoon have been optimized to obtain the minimum total system travel time after reaching its destination. For the configuration of Newell's car-following model, we set the rear-to-end distance $d_0 = 2\ m$ and τ is variable at intersection regions between 2 s to 0 s with the step size of reaction time change is 0.2 s. There are 5 tightly coupled autonomous and connected vehicles along a one-lane roadway. Fig. 13 shows a typical vehicle trajectory as a black dash line and optimal AVs trajectories as solid blue lines.

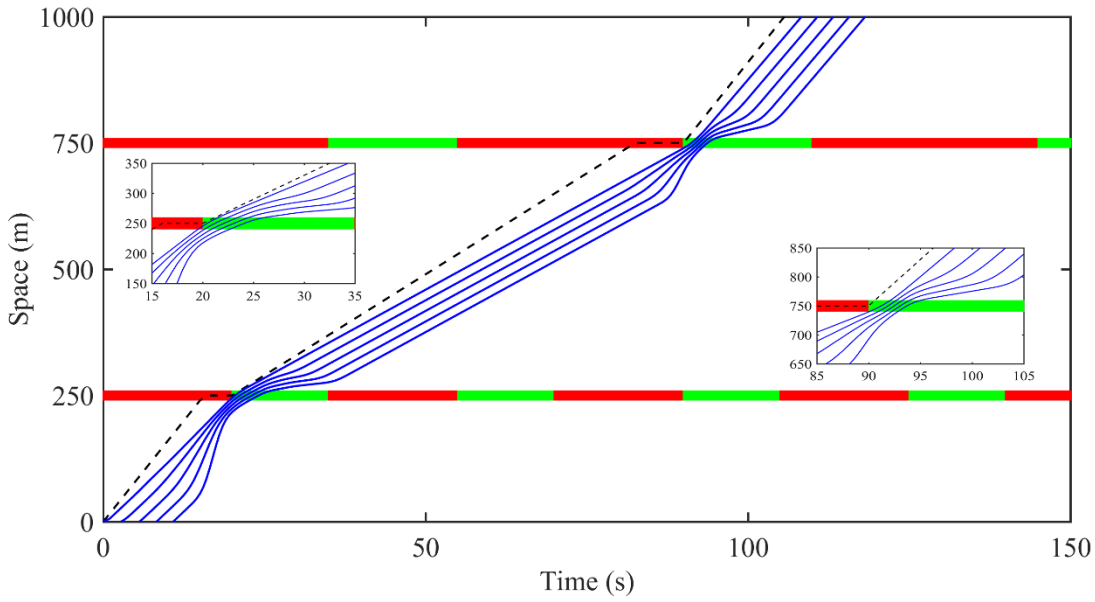

a) Illustration without speed limit in transition process

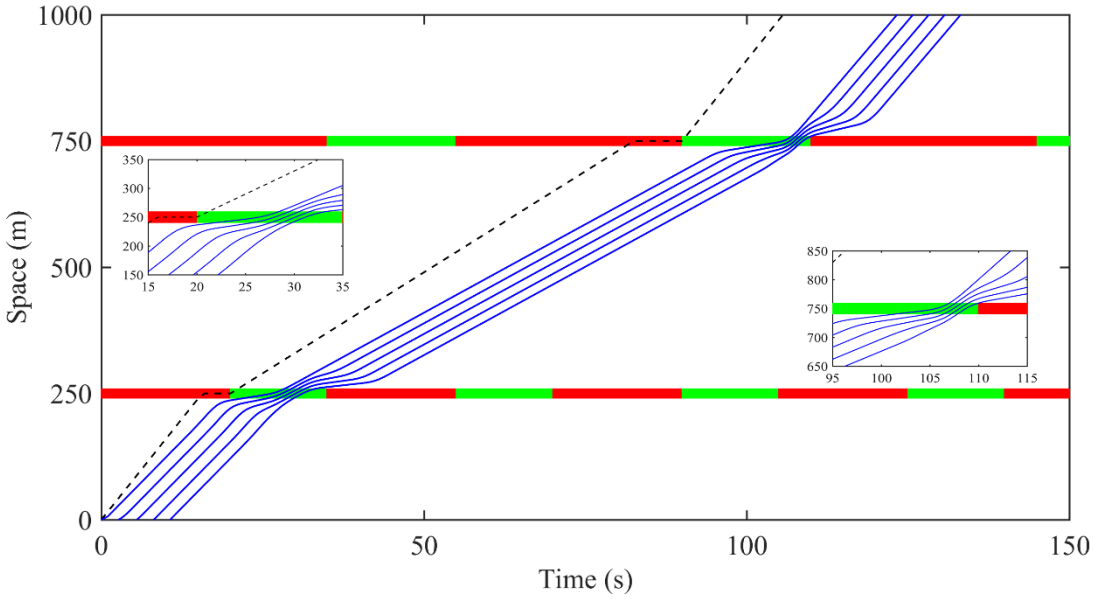

b) Enforcing speed limit for leading vehicle in transition process

Fig. 13: Optimal vehicle trajectories by using mode '1+m(w)'

Trajectories and speed of AVs can be changed to find optimal solution with minimum system level emission objectives or energy consumption based on the corresponding speed-related polynomial cost function (e.g. Abdul Aziz and Ukkusuri, 2012). While human-driving vehicles have to wait at intersections (shown was dash lines), all AVs can pass through the intersections without waiting by reducing reaction time and optimized speed along the journey. Since the reaction time and speed have been changed at different segments to find the optimal solution, maximum service rates can be also calculated analytically at different locations. To derive more practically useful capacity estimation results under different communication standards, a more systematically designed study should be conducted to provide the guidelines using realistic settings and real-world geometry features. In addition, the last vehicle in Fig. 13(a) appears to violate the speed limit. As noted in section 2.2, it is possible for the following vehicle when the reaction time is changeable in the state transition process. However, as a control variable, the speed of lead vehicle cannot exceed the maximum speed in this mode. Different simulation results can be obtained by assigning different settings such as enforcing speed limit for leading vehicle in transition process in Fig. 13(b). While the last vehicle in the platoon can speed up to catch up leading vehicle in Fig. 13(a), the last vehicle keeps its speed and the leading vehicles slow down in transition process in Fig. 13(b).

It should be remarked that, the solution obtained by DP may be just one of optimal solutions to reach system-level minimal travel cost. The result with an optimal reaction time greater than the minimum reaction time can improve the safety, to some extent, when using an unchanged minimum reaction time can also reach the minimal system cost.

5. 2 Platoon Analysis by Using Mode "1 + M" for Automated Vehicles with Surrounding Obstacles

One challenge of deploying autonomous vehicles in the real world is to consider the influence from moving obstacles (e.g. human-driving vehicle) and static obstacles (e.g. stuffs left unintentionally on roads). In this section, we perform experiments to demonstrate how to optimize vehicle trajectories for avoiding moving obstacles, which can be detected in real time by sensors from autonomous vehicles. Since the mode is still at "1+m", the lead autonomous vehicle is just under control and its following autonomous vehicles have a fixed reaction time and adjust their trajectory based on the change of the lead vehicle.

Fig. 14 shows AV's trajectories by using mode (1+m) with surrounding real-world human driving car trajectories obtained from the NGSIM project for I-80 in California (USDOT, 2006). Trajectories of human operated vehicles on lane 1 and lane 2 have been used for experiments where identification numbers are 1247, 1253, 1255, 1284, 1297, 1306 and 1325; 3360, 417, 436, 447, 448, 459, 469, 472, 488, 494 and 507 respectively. The total length of the road segment is 500 meters and the speed limit is 70 miles per hour. For the configuration of Newell's car-following model, we set $d_0 = 2m$ and τ is fixed as 0.5 to show mixed traffic condition trajectories. Hypothetical layout of experiments has been illustrated in Fig. 14(a), human operated vehicles trajectories have been shown in Fig. 14(b). Further experiments only for lane 2, human operated vehicles which identification numbers are 3360 and 488 have been excluded. AVs and human operated vehicles trajectories from origin to destination and zooming view of highlighted region in Fig. 14(c) have been shown Fig. 14(c) and Fig. 14(d), respectively. Table 5 shows the maximum MSR values in mixed traffic condition for lane 1. As can be seen, MSR increases as reaction times decrease. Also for lane 2, in heavy traffic condition, MSR increases 50% by excluding only two human operated vehicles.

Table 5. MSR (vphpl) by using different reaction times with moving obstacles

Human-operated vehicles	Human-operated and AVs with different reaction time (s)			
	$\tau = 1.5$ s	$\tau = 1$ s	$\tau = 0.5$ s	$\tau = 0$ s
458	1047	1309	1898	3665

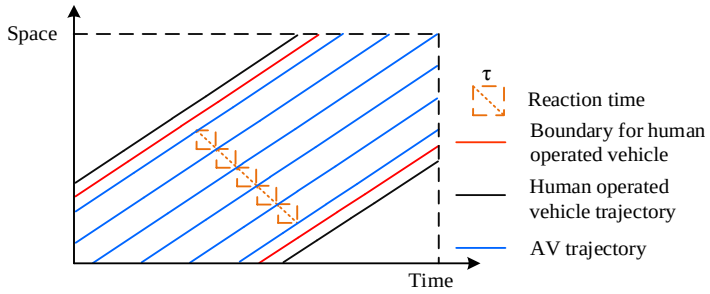

(a) Hypothetical layout of experiments

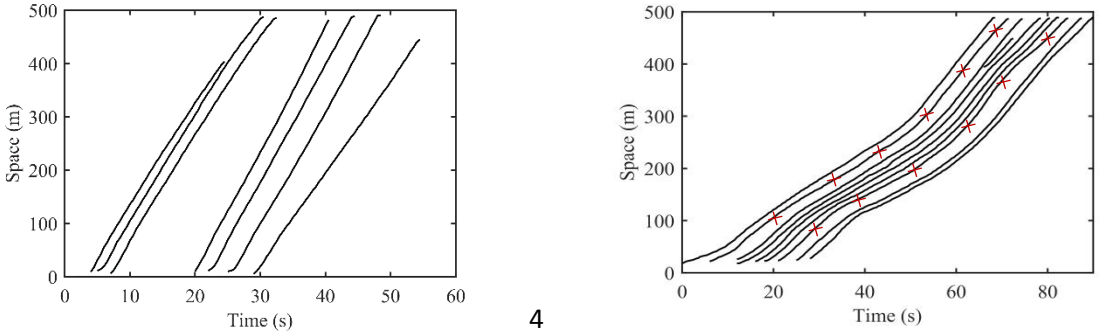

(b) Human-operated vehicle trajectories for NGSIM data 101 lane 1 and 2, respectively

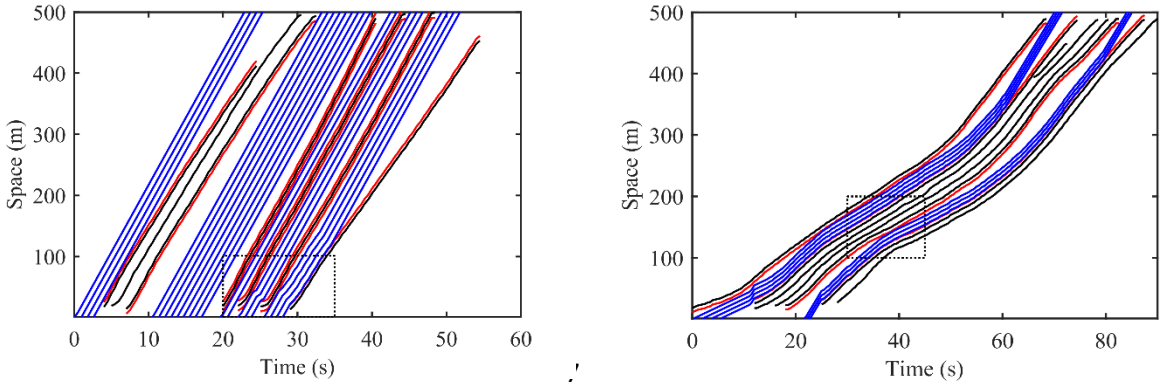

(c) Mixed traffic conditions when reaction time equals 0.5 s for lane 1 and 2, respectively

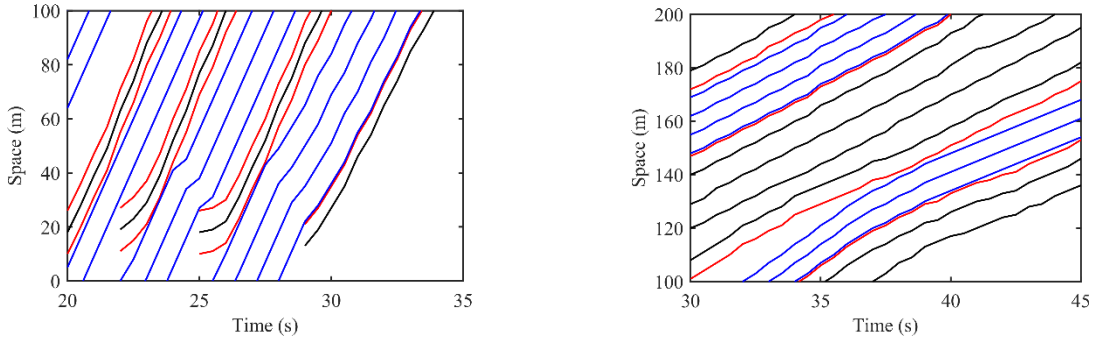

(d) Zooming view of mixed traffic conditions which highlighted in (c) for lane 1 and 2, respectively

Fig. 14. AV's trajectories by using mode (1+m) with real human driving car trajectories obtained from NGSIM Data

5.3. Integer Programming Model

The proposed mathematical model defined by Eq. (20-23) is applied in the following tests, where autonomous vehicles move along a one-lane roadway with three segments (AB, BC, and CD) and total 30 space units (e.g., 2 or 3 meters). Each segment has one specific communication facility, which indicates that each vehicle can only have one particular reaction time to its leading vehicle. In these tests, the total time horizon is 40 time intervals (e.g., 20s or 40 s). Each vehicle is assumed to have four speed values to be selected at each time stamp, including 0, 1 space unit, 2 space units, and 3 space units. The minimum spacing d_{jam} between two autonomous vehicles is assumed as 2 space units. The reaction and operation times w of segments AB, BC, and CD are 1 time unit, 2 time units and 3 time units, respectively. Tests 1 and 2 focus on two autonomous vehicles in order to perform the sensitivity of departure time with the impact on system-wide travel times. In all tests, all vehicles depart at node/space 1 and should arrival at node 30.

When departure times of vehicles 1 and 2 are 1 and 4, respectively, the problem is directly solved in GAMS based on our proposed mathematical model. Fig.15(a) shows the optimized vehicles' trajectories. It is expected that vehicle 1 can always move in speed limit as 3 space units at each time interval in this discretized space-time network. However, the vehicle reduces its speed at time 8, because if it moves in speed limit, it will reach at node/space 31 after 10 time units rather than node 30 as the destination due to the discretization property of space-time networks. The red rectangle defines the incompatible zone for the following vehicle (vehicle 2) when its reaction time is 3 time units. As shown in Fig.15(a), at the beginning, vehicle 1 stays at the incompatible zone of vehicle 2 if vehicle 2 has communication time of 3 time units, which indicates that vehicle 2 should reduce its speed to ensure there is no conflict with vehicle 1 after node 20 (at segment CD). As a result, the total system travel time is 21 where vehicles 1 and 2 have travel time of 10 and 11, respectively. The shock wave is not obviously found in the result. One possible reason is that the solution above is just one of multiple optimal solutions for our system optimal problem, so vehicles could reduce or increase its speed at different locations with a same minimum system travel time. In other words, once all vehicles can be controlled as autonomous vehicles, vehicles can reduce its speed at any locations before the bottleneck and then drive with a higher speed to pass the following roadway, and it is possible that traditional shock wave happened at bottlenecks will not be obviously observed in future.

In Test 2, the departure time of vehicle 2 is changed to be 3. Then the final optimization result from GAMS is shown in Fig.15(b). It can be also observed that vehicle 2 needs to reduce its speed to accommodate the high communication time at segment CD. The total travel time will increase to 22 instead of 21 in Test 1.

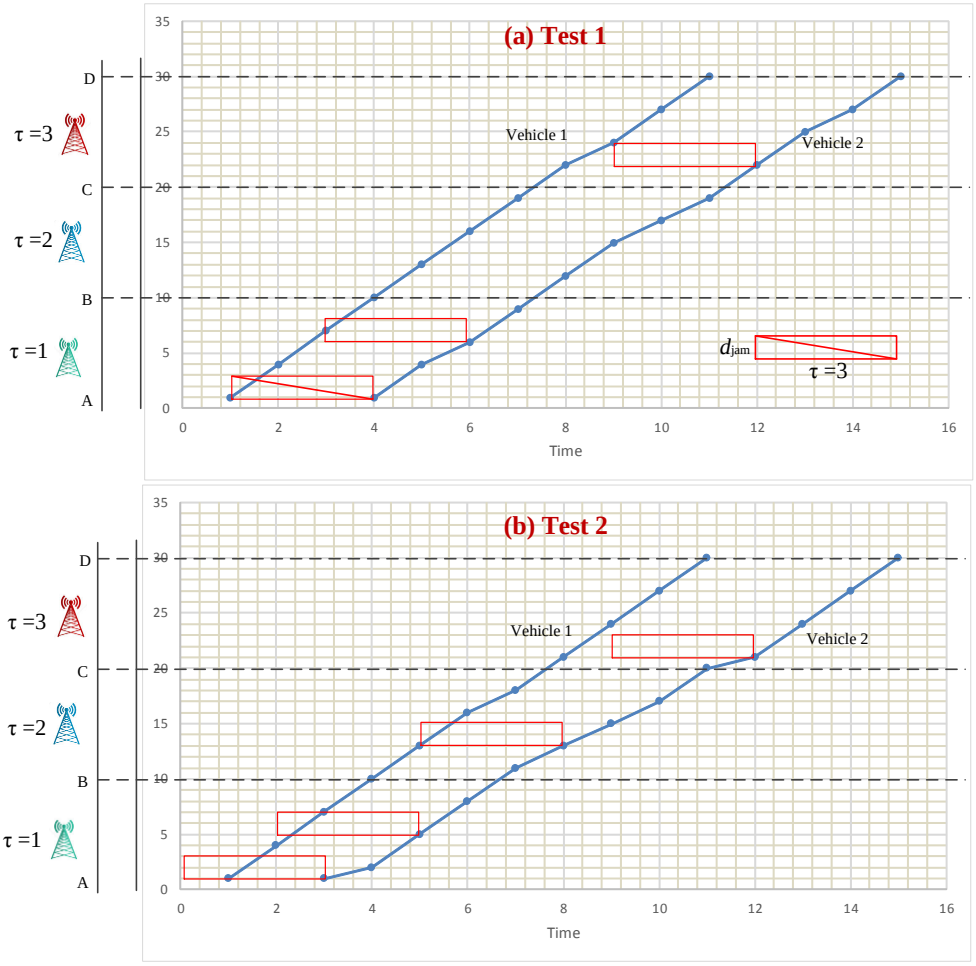

Fig.15. Optimized vehicle trajectories of tests 1 and 2 in discretized space-time grid from integer programming model

Further, we consider Test 3 with 5 autonomous vehicles, whose departure times are at 1st, 3rd, 6th, 9th, and 11en time interval. The optimization result from GAMS (with CPLEX solver) shows that vehicle 5 waits and moves with a high speed at segment AB. As remarked in Test 2, the optimization result could be one of multiple optimal solutions, so vehicle 5 can also drive with medium speeds at segment AB without violating car-following constraints. The model statistics of three tests, including number of equations, number of variables, optimal objective value, and computation time, are listed in Table 6.

Table 6. Model statistics of three tests with 30 by 40 space time grid based on GAMS with CPLEX solver

	number of equations	number of binary variables	objective value (time unit)	computation time (second)
Test 1 (2 vehicles)	6,083	8,972	21	1.3
Test 2 (2 vehicles)	6,083	8,972	22	1.4
Test 3 (5 vehicles)	17,006	22,430	65	2.8

6. Conclusion

The main focus of this paper is to present a novel control strategy for autonomous and connected vehicles. This study constructs a family of efficient optimization models and algorithms to embed vehicle kinematics and minimum safe distance between consecutive following vehicles by using extended Newell's simplified car-following model. The main advantage of the proposed model is to enhance the service rate by adjusting vehicle trajectory speed and system level platoon reaction time at critical bottlenecks. Unlike similar control strategies, which handle only closed boundary conditions, the proposed model solves efficiently semi-open boundary conditions by using integer programming and dynamic programming models with travel time, throughput and fuel consumption optimization objectives. The two aspects namely (i) adjustment of system level reaction time in discretized space-time-reaction time network and (ii) focusing on the optimality of system through controlling simultaneously all vehicles in the platoon, contribute new knowledge to the existing vehicle trajectory optimization studies.

The results of numerical experiments have revealed efficiency of controlling reaction time as a new control variable, and increasing system level flexibility and optimality by forming vehicle platoons adaptively at critical bottlenecks. Also, these results give projections for communication connectivity considering team based safety when reaction time dynamically changes under communication support conditions. Both approaches for integer programming and dynamic programming under typical time-dependent bottleneck scenarios are examined to show the benefits of optimizing AVs trajectories with achievement of desired goals. Finally, through the numerical experiments for configuring platoon level reaction time under complex driving conditions by using real world trajectories data, it can be noted that multiple AVs increase the service rate under supported communication conditions. Future work will mainly focus on (i) using backward and forward DP algorithms to better refine the feasible space prim and iteratively search the feasible ending states for ultimate optimal solutions, (ii) better selecting the discretization granularity for our multi-dimensional discretized networks, (iii) smoothing vehicle trajectories generated by Newell's car-following model, and (iv) developing control models for the formation of swarms consisting of multiple AVs in a large scale application.

Acknowledgements

The second author has received the financial support of the Scientific and Technological Research Council of Turkey (TÜBİTAK) under reference number 1059B141500634 and entitled as "Developing Agent-Based Traffic Simulation System and Congestion Algorithm". The last author is partially funded by National Science Foundation–United States under NSF Grant No. CMMI 1538105 "Collaborative Research: Improving Spatial Observability of Dynamic Traffic Systems through Active Mobile Sensor Networks and Crowdsourced Data", and CMMI 1663657 "Real-time Management of Large Fleets of Self-Driving Vehicles Using Virtual Cyber Tracks". The authors would like to thank Jeffrey Taylor at University of Utah for his valuable comments.

Appendix A. Dynamic programming algorithms for modes "1" and "1+1"

Mode ("1")

The DP-based optimization algorithm for mode (1) is described as below:

We denote D as the total distance under consideration, d^{max}as the maximum distance one vehicle can travel at one time step, $L(t,x(t))$ as the value function of state $x(t)$ at t, $t \in [0,T], x \in [0,D]$, d^{max}as the maximum distance one vehicle can travel at one time step (equal to v_{max} in this paper), and the initial $L(t,x(t))$ values are all positive infinity.

```
// initialization
L(t, x_1(t)) := +∞;  // value of state (x_1(t))
L(0, x_1(0)) := 0;
for t = 0 to T do
    for x_1(t) = 0 to D  (within the feasible range) do
        for x_1(t+1) = x_1(t) to min{D, x_1(t) + d^max} do
            if x_1(t) and x_1(t+1) are within feasible space-time regions;
            and  L(t, x_1(t)) + c[x_1(t), x_1(t+1)] < L(t+1, x_1(t+1))
            then L(t+1, x_1(t+1)) = L(t, x_1(t)) + c[x_1(t), x_1(t+1)];
        endfor;
    endfor;
endfor;
```

After all iterations, search the corresponding time index with the minimal label cost at D and trace back to get the optimal vehicle trajectory. Total cost $(t = T^*, x = D) = \min_t\{\mathrm{L(t, x = D)}\}$, where T^* is the time index leading to the minimum cost value at distance D.

Mode ("1+1")

Denote $L(t, x_1(t), x_2(t+\tau))$ as the value function of state$(x_1(t), x_2(t+\tau))$ at t, $t \in [0, T], x \in [0, D]$.

```
// initialization
L(t, x_1(t), x_2(t+τ)) := +∞;  // value of state (x_1(t), x_2(t+τ))
L(t, x_1(0), x_2(0+τ)) := 0;
for t = 0 to T do
    for x_1(t) = 0 to D do
        for x_2(t+τ) = 0 to x_1(t) − d do
            for x_1(t+1) = x_1(t) to x_1(t) + d^max do
                for x_2(t+τ+1) = x_2(t+τ) to min{x_1(t+1) − d, x_2(t+τ) + d^max} do
                    if  x_1(t), x_1(t+1), x_2(t+τ), x_2(t+τ+1) are within feasible space-time regions;
                    and L(t, x_1(t), x_2(t+τ)) + c(x_1(t), x_1(t+1), x_2(t+τ), x_2(t+τ+1)) < L(t+1, x_1(t+1), x_2(t+τ+1))
                    then  L(t+1, x_1(t+1), x_2(t+τ+1)) = L(t, x_1(t), x_2(t+τ)) + c(x_1(t), x_1(t+1), x_2(t+τ), x_2(t+
                          τ+1));
                endfor;
            endfor;
        endfor;
    endfor;
endfor;
```

Because the final arrival times at the space boundary are not fixed, we need to search the corresponding time indices of two vehicles with the minimal label cost at D and trace back to obtain the optimal vehicle trajectory of each vehicle respectively.

Appendix B. Possible Extension to Multi-Platoon Merging Control

Vehicle merging on ramps is a major traffic flow problem on highways which causes congestion, speed breakdown and traffic flow oscillations (Chen et al., 2014; Sun et al., 2014). The merging process in human operated vehicle environment consists of the following three steps: choosing possible gap for the adjacent target lane, adjusting speed, and performing required maneuvers (Ntousakis et al., 2016). As a simple conceptual illustration, the merging process in AV environment can be performed with satisfying desired objectives and ensuring safety constraints. We can provide optimized solution for merging process by controlling all AVs in on-ramp and mainstream, and by defining different reaction times for platoon level (τ_p) and system level (τ_s). As shown in Fig. 16, there are two different platoons before merging consisting of 3 and 2 AVs, respectively. In this merging process, the system level reaction time is symmetrically adjusted to meet distance headway constraints between vehicles from two different platoons. In our illustrative example, the merging point is assumed to be the end of the acceleration lane.

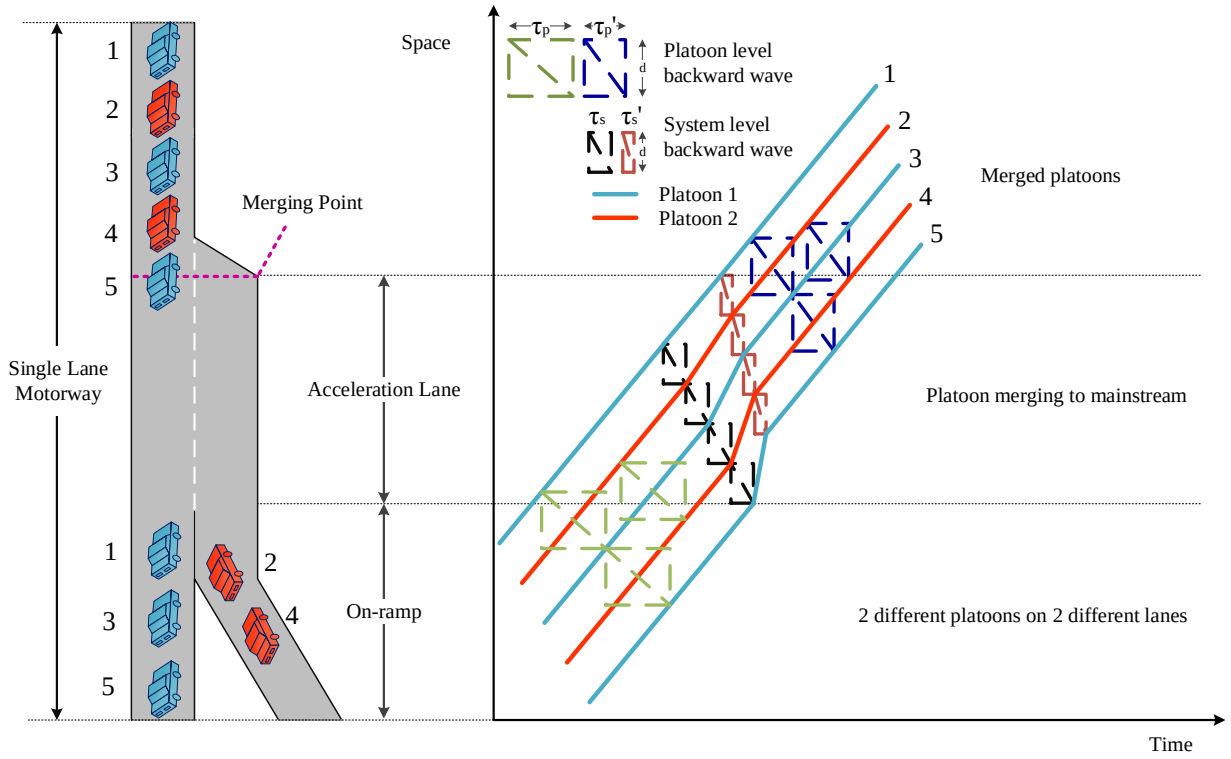

Fig. 16. Illustration of merging process by using multi-platoon formation control

References

Abdul Aziz, H.M. , Ukkusuri, S.V. (2012). Integration of environmental objectives in a system optimal dynamic traffic assignment model. Comput. Aided Civil Infrastruct. Eng. 27 (7), 494–511.

Ahn, S., Cassidy, M. J., & Laval, J. (2004). Verification of a simplified car-following theory. Transportation Research Part B: Methodological, 38(5), 431-440.

Akyildiz, I. F., Nie, S., Lin, S. C., & Chandrasekaran, M. (2016). 5G roadmap: 10 key enabling technologies. *Computer Networks*, *106*, 17-48.

Alvarez, L., & Horowitz, R. (1999). Safe platooning in automated highway systems part I: Safety regions design. Vehicle System Dynamics, 32(1), 23-55.

Askari, A., Farias, D., Kurzhanskiy, K., Varaiya, P. (2017). Effect of Adaptive and Cooperative Adaptive Cruise Control on Throughput of Signalized Arterials. arXiv:1703.01657

Bang, S., Ahn, S. (2017). Platooning Strategy for Connected and Autonomous Vehicles: Transition From Light Traffic. the 96th 10 Transportation Research Board Annual Meeting, Paper ID: 17-02010.

Bai, F., & Krishnan, H. (2006, September). Reliability analysis of DSRC wireless communication for vehicle safety applications. In 2006 IEEE Intelligent Transportation Systems Conference (pp. 355-362). IEEE.

Balch, T., & Arkin, R. C. (1998). Behavior-based formation control for multirobot teams. IEEE transactions on robotics and automation, 14(6), 926-939.

Betts, J. T. (1998). Survey of numerical methods for trajectory optimization. Journal of guidance, control, and dynamics, 21(2), 193-207.

Bose, A., & Ioannou, P. (1999). Analysis of traffic flow with mixed manual and semi-automated vehicles. In American Control Conference, 1999. Proceedings of the 1999 (Vol. 3, pp. 2173-2177). IEEE.

Bose, A., & Ioannou, P. A. (2003). Analysis of traffic flow with mixed manual and semiautomated vehicles. IEEE Transactions on Intelligent Transportation Systems, 4(4), 173-188.

Bradley, S., Hax, A., & Magnanti, T. (1977). Applied mathematical programming. Chapter 11.

Chandler, R. E., Herman, R., & Montroll, E. W. (1958). Traffic dynamics: studies in car following. Operations research, 6(2), 165-184.

Chen, J., Sun, D., Yang, J., & Chen, H. (2009). A leader-follower formation control of multiple nonholonomic mobile robots incorporating receding-horizon scheme. The International Journal of Robotics Research.

Chen, X. M., Li, Z., Li, L., & Shi, Q. (2014). A traffic breakdown model based on queueing theory. *Networks and Spatial Economics*, *14*(3-4), 485-504.

Chen, Y. Q., & Wang, Z. (2005, August). Formation control: a review and a new consideration. In Intelligent Robots and Systems, 2005. (IROS 2005). 2005 IEEE/RSJ International Conference on (pp. 3181-3186). IEEE.

Cheng, X., Chen, C., Zhang, W., & Yang, Y. (2017). 5G-Enabled Cooperative Intelligent Vehicular (5GenCIV) Framework: When Benz Meets Marconi. *IEEE Intelligent Systems*, *32*(3), 53-59.

De Wit, C.C., Sordalen, O.J. (1992). Exponential stabilization of mobile robots with nonholonomic constraints. IEEE transactions on automatic control, 37(11), 1791-1797.

Egerstedt, M. B., & Hu, X. (2001). Formation constrained multi-agent control.

Flint, M., Polycarpou, M., & Fernandez-Gaucherand, E. (2002). Cooperative path-planning for autonomous vehicles using dynamic programming. In Proceedings of the IFAC 15th Triennial World Congress (pp. 1694-1699).

Forbes, T. W. (1963). Human factor considerations in traffic flow theory. Highway Research Record, (15).

Forbes, T. W., Zagorski, H. J., Holshouser, E. L., & Deterline, W. A. (1958). Measurement of driver reactions to tunnel conditions. In Highway Research Board Proceedings (Vol. 37).

Gong, S., Shen, J. and Du, L., (2016). Constrained optimization and distributed computation based car following control of a connected and autonomous vehicle platoon. Transportation Research Part B: Methodological, 94, 314-334.

Grøtli, E. I., & Johansen, T. A. (2012). Path planning for UAVs under communication constraints using SPLAT! and MILP. Journal of Intelligent & Robotic Systems, 65(1-4), 265-282.

Grøtli, E. I., & Johansen, T. A. (2016). Motion-and Communication-Planning of Unmanned Aerial Vehicles in Delay Tolerant Network using Mixed-Integer Linear Programming. Modeling, Identification and Control, 37(2), 77.

Guo, Y., & Parker, L. E. (2002). A distributed and optimal motion planning approach for multiple mobile robots. In Robotics and Automation, 2002. Proceedings. ICRA'02. IEEE International Conference on (Vol. 3, pp. 2612-2619). IEEE.

Hamdar, S. H., Treiber, M., & Mahmassani, H. S. (2009). Calibration of a stochastic car-following model using trajectory data: exploration and model properties. In Transportation Research Board 88th Annual Meeting (No. 09-3450).

He, X., Liu, H. X., & Liu, X. (2015). Optimal vehicle speed trajectory on a signalized arterial with consideration of queue. Transportation Research Part C: Emerging Technologies, 61, 106-120.

Hoogendoorn, S., Hoogendoorn, R., & Daamen, W. (2011). Wiedemann revisited: new trajectory filtering technique and its implications for car-following modeling. Transportation Research Record: Journal of the Transportation Research Board, (2260), 152-162.

Horowitz, R., & Varaiya, P. (2000). Control design of an automated highway system. Proceedings of the IEEE, 88(7), 913-925.

Hu, J., Shao, Y., Sun, Z., Wang, M., Bared, J., & Huang, P. (2016). Integrated optimal eco-driving on rolling terrain for hybrid electric vehicle with vehicle-infrastructure communication. Transportation Research Part C: Emerging Technologies, 68, 228-244.

Intel, 2017. The 5G-Autonomous Driving Connection. <https://newsroom.intel.com/wp-content/uploads/sites/11/2017/05/why-5G-for-ad-fact-sheet.pdf> (accessed 05.11.2017).

Ioannou, P. A. (1994). Activity D: Lateral and longitudinal control analysis. Final Report.

Jensen, P. A., & Bard, J.F. (2003). Operations research models and methods. Vol. 1. John Wiley & Sons Incorporated. Chapter 20.

Jia, D., & Ngoduy, D. (2016a). Platoon based cooperative driving model with consideration of realistic inter-vehicle communication. Transportation Research Part C: Emerging Technologies, 68, 245-264.

Jia, D., & Ngoduy, D. (2016b). Enhanced cooperative car-following traffic model with the combination of V2V and V2I communication. Transportation Research Part B: Methodological, 90, 172-191.

Kanayama, Y., Kimura, Y., Miyazaki, F., Noguchi, T. (1990). A stable tracking control method for an autonomous mobile robot. In Robotics and Automation, IEEE International Conference, 384-389.

Katrakazas, C., Quddus, M., Chen, W. H., & Deka, L. (2015). Real-time motion planning methods for autonomous on-road driving: State-of-the-art and future research directions. Transportation Research Part C: Emerging Technologies, 60, 416-442.

Kesting, A., Treiber, M., Helbing, D. (2010). Connectivity statistics of store-and-forward inter-vehicle communication. IEEE Trans. Intell. Transp. Syst. 11, 172–181

Kim, J., & Mahmassani, H. (2011). Correlated parameters in driving behavior models: car-following example and implications for traffic microsimulation. Transportation Research Record: Journal of the Transportation Research Board, (2249), 62-77.

Kometani, E., & Sasaki, T. (1958). On the stability of traffic flow (report-I). Journal of Operations Research Japan, 2(1), 11-26.

Kometani, E., & Sasaki, T. (1959). A safety index for traffic with linear spacing. Operations research, 7(6), 704-720.

Kometani, E. & Sasaki, T. (1961), Dynamic Behavior of Traffic with a Non-liner Spacing-Speed Relationship, Theory of Traffic Flow Symposium Proceeding, Pages 105-119.

Kreutz, D., Ramos, F. M., Verissimo, P. E., Rothenberg, C. E., Azodolmolky, S., & Uhlig, S. (2015). Software-defined networking: A comprehensive survey. Proceedings of the IEEE, 103(1), 14-76.

Laval, J. A., & Leclercq, L. (2010). A mechanism to describe the formation and propagation of stop-and-go waves in congested freeway traffic. Philosophical Transactions of the Royal Society of London A: Mathematical, Physical and Engineering Sciences, 368(1928), 4519-4541.

LaValle, S. M. (2006). Planning algorithms. Cambridge university press.

Liu, J., & Zhou, X. (2016). Capacitated transit service network design with boundedly rational agents. Transportation Research Part B: Methodological, 93, 225-250.

Lioris, J., Pedarsani, R., Tascikaraoglu, F.Y. and Varaiya, P. (2017). Platoons of connected vehicles can double throughput in urban roads. Transportation Research Part C: Emerging Technologies, 77, 292-305.

Lu, C. C., Liu, J., Qu, Y., Peeta, S., Rouphail, N. M., & Zhou, X. (2016). Eco-system optimal time-dependent flow assignment in a congested network. Transportation Research Part B: Methodological, 94, 217-239.

Ma, J., Li, X., Zhou, F., Hu, J., & Park, B. B. (2016). Parsimonious shooting heuristic for trajectory design of connected automated traffic part II: Computational issues and optimization. Transportation Research Part B: Methodological.

Mahmassani, H. S. (2016). 50th Anniversary Invited Article—Autonomous Vehicles and Connected Vehicle Systems: Flow and Operations Considerations. Transportation Science, 50(4), 1140-1162.

McNaughton, M. (2011). Parallel algorithms for real-time motion planning, PhD dissertation.

Miao, Z., Wang, Y. (2015). Adaptive Control for Simultaneous Stabilization and Tracking of Unicycle Mobile Robots. Asian Journal of Control, 17(6), 2277-2288.

Milanés, V., & Shladover, S. E. (2014). Modeling cooperative and autonomous adaptive cruise control dynamic responses using experimental data. Transportation Research Part C: Emerging Technologies, 48, 285-300.

Murray, R. M. (2007). Recent research in cooperative control of multivehicle systems. Journal of Dynamic Systems, Measurement, and Control, 129(5), 571-583.

Munigety, C. R., Gupta, P. A., Gurumurthy, K. M., Peeta, S., and Mathew, T. V. (2016). Vehicle- type Dependent Car following Model Using Spring-mass-damper Dynamics for Heterogeneous Traffic. the 95th Transportation Research Board Annual Meeting.

National Automated Highway System Consortium(NAHSC), Milestone 2 Reporter (1996) Hard Braking Safety Analysis Method and Detailed Results, Appendix J, 17.

Newell, G. F. (1993). A simplified theory of kinematic waves in highway traffic, part I: General theory. Transportation Research Part B: Methodological, 27(4), 281-287.

Newell, G. F. (2002). A simplified car-following theory: a lower order model. Transportation Research Part B: Methodological, 36(3), 195-205.

Ntousakis, I. A., Nikolos, I. K., & Papageorgiou, M. (2016). Optimal vehicle trajectory planning in the context of cooperative merging on highways. *Transportation Research Part C: Emerging Technologies*, *71*, 464-488.

Paden, B., Cap, M., Yong, S. Z., Yershov, D., & Frazzoli, E. (2016). A Survey of Motion Planning and Control Techniques for Self-driving Urban Vehicles. arXiv preprint arXiv:1604.07446.

Pipes, L.A. (1953), An Operational Analysis of Dynamics, Journal of Applied Physics, Vol.24, No.3, Pages 274-287.

Przybyla, J., Taylor, J., Jupe, J., & Zhou, X. (2015). Estimating risk effects of driving distraction: a dynamic errorable car-following model. Transportation Research Part C: Emerging Technologies, 50, 117-129.

Reuschel, A. (1950), Vehicle Movements in a Platoon, Oesterreichisches Ingenieur-Archir, Vol.4, Pages 193-215.

Richards, A., Bellingham, J., Tillerson, M., & How, J. (2002, August). Coordination and control of multiple UAVs. In AIAA guidance, navigation, and control conference, Monterey, CA.

Roncoli, C., Papageorgiou, M., & Papamichail, I. (2015a). Traffic flow optimization in presence of vehicle automation and communication systems–Part I: A first-order multi-lane model for motorway traffic. Transportation Research Part C: Emerging Technologies, 57, 241-259.

Roncoli, C., Papageorgiou, M., & Papamichail, I. (2015b). Traffic flow optimization in presence of vehicle automation and communication systems–Part II: Optimal control for multi-lane motorways. Transportation Research Part C: Emerging Technologies, 57, 260-275.

Schouwenaars, T., De Moor, B., Feron, E., & How, J. (2001, September). Mixed integer programming for multi-vehicle path planning. In Control Conference (ECC), 2001 European (pp. 2603-2608). IEEE.

Stentz, A. (1994). Optimal and efficient path planning for partially-known environments. In Robotics and Automation, 1994. Proceedings., 1994 IEEE International Conference on (pp. 3310-3317). IEEE.

Sun, J., Ouyang, J., Yang, J. (2014). Modeling and analysis of merging behavior at expressway on-ramp bottlenecks. Transp. Res. Rec.: J. Transp. Res. Board 2421, 74–81.

Sun, X., & Cassandras, C. G. (2016). Optimal dynamic formation control of multi-agent systems in constrained environments. Automatica, 73, 169-179.

Talebpour, A., & Mahmassani, H. S. (2015). Influence of Autonomous and Connected Vehicles on Stability of Traffic Flow. In Transportation Research Board 94th Annual Meeting (No. 15-5971).

Taylor, J., Zhou, X., Rouphail, N. M., & Porter, R. J. (2015). Method for investigating intradriver heterogeneity using vehicle trajectory data: a dynamic time warping approach. Transportation Research Part B: Methodological, 73, 59-80.

Treiber, M., Hennecke, A., & Helbing, D. (2000). Congested traffic states in empirical observations and microscopic simulations. Physical review E, 62(2), 1805.

Urmson, C., Anhalt, J., Bagnell, D., Baker, C., Bittner, R., Clark, M. N., ... & Gittleman, M. (2008). Autonomous driving in urban environments: Boss and the urban challenge. Journal of Field Robotics, 25(8), 425-466.

US Department of Transportation (USDOT), 2006. NGSIM – Next Generation Simulation. <http://ops.fhwa.dot.gov/trafficanalysistools/ngsim.htm> (accessed 04.02.2017).

Varaiya, P. (1993). Smart cars on smart roads: problems of control. IEEE Transactions on automatic control, 38(2), 195-207.

Ward, J. D. (1997). Step by Step to an Automated Highway System—And Beyond. In Automated Highway Systems (pp. 73-91). Springer US.

Wu, X., He, X., Yu, G., Harmandayan, A., & Wang, Y. (2015). Energy-optimal speed control for electric vehicles on signalized arterials. IEEE Transactions on Intelligent Transportation Systems, 16(5), 2786-2796.

Xu, L., Wang, L. Y., Yin, G., & Zhang, H. (2014). Communication information structures and contents for enhanced safety of highway vehicle platoons. IEEE Transactions on Vehicular Technology, 63(9), 4206-4220.

Yanakiev, D. and Kanellakopoulos, I. (1998). A simplified framework for string stability analysis of automated vehicles. Vehicle System Dynamics, Vol. 30, 375-405.

Zhou, F., Li, X., & Ma, J. (2017). Parsimonious shooting heuristic for trajectory design of connected automated traffic part I: Theoretical analysis with generalized time geography, Transportation Research Part B: Methodological. 95, 394-420.

Zhou L, Tong L, Chen J, Tang J, Zhou X. (2017). Joint optimization of high-speed train timetables and speed profiles: A unified modeling approach using space-time-speed grid networks. Transportation research part B : Methodological 97, 157-181.